

Learning to Simulate: Generative Metamodeling via Quantile Regression

L. Jeff Hong

School of Management and School of Data Science, Fudan University, Shanghai 200433, China, hong_liu@fudan.edu.cn

Yanxi Hou

School of Data Science, Fudan University, Shanghai 200433, China, yxhou@fudan.edu.cn

Qingkai Zhang

School of Management, Fudan University, Shanghai 200433, China, 22110690021@m.fudan.edu.cn
Department of Management Sciences, City University of Hong Kong, Kowloon, Hong Kong SAR, China

Xiaowei Zhang

Department of Industrial Engineering and Decision Analytics, The Hong Kong University of Science and Technology, Clear Water Bay, Hong Kong SAR, China, xiaoweiz@ust.hk

Stochastic simulation models, while effective in capturing the dynamics of complex systems, are often too slow to run for real-time decision-making. Metamodeling techniques are widely used to learn the relationship between a summary statistic of the outputs (e.g., the mean or quantile) and the inputs of the simulator, so that it can be used in real time. However, this methodology requires the knowledge of an appropriate summary statistic in advance, making it inflexible for many practical situations. In this paper, we propose a new metamodeling concept, called *generative metamodeling*, which aims to construct a “fast simulator of the simulator”. This technique can generate random outputs substantially faster than the original simulation model, while retaining an approximately equal conditional distribution given the same inputs. Once constructed, a generative metamodel can instantaneously generate a large amount of random outputs as soon as the inputs are specified, thereby facilitating the immediate computation of any summary statistic for real-time decision-making. Furthermore, we propose a new algorithm—quantile-regression-based generative metamodeling (QRGMM)—and study its convergence and rate of convergence. Extensive numerical experiments are conducted to investigate the empirical performance of QRGMM, compare it with other state-of-the-art generative algorithms, and demonstrate its usefulness in practical real-time decision-making.

Key words: generative metamodeling, simulation with covariates, real-time decision-making

1. Introduction

Simulation is a powerful tool for modeling and analysis of real-world systems, and has been widely used across many practical situations (Banks et al. 2009). However, running simulation models

This research is partially supported by the Laboratory for AI-Powered Financial Technologies in Hong Kong, while LJH and QZ served as visiting scientists of the lab.

can be time-consuming, especially for complex systems. Therefore, in practice, simulation has primarily been used as a design tool, where sufficient time is usually available to conduct simulation experiments to evaluate, improve or optimize the design of a system. In recent years, to further harness its modeling capability, there is an increasing need to use simulation for real-time decision-making. This is evident in areas such as digital twins in manufacturing and real-time antenna control in telecommunications. The challenge lies in applying slow simulations to support fast, real-time decision-making processes, where a part of the simulation input variables—which are called covariates—are observed in real time.

Covariates pose a significant challenge for real-time decision-making with simulation, because their exact values are unknown in advance. Many recent studies have focused on using statistical learning methods to build predictive models to capture the relationship between the covariates and a summary statistic of the simulation outputs. Once this relationship is learned, the summary statistic can be quickly predicted using the predictive models when the covariates are observed, thereby accelerating the use of simulation for decision-making. Hong and Jiang (2019) summarized the key features of these studies and proposed an offline-simulation-online-application (OSOA) framework. Within this framework, one uses offline simulation experiments to build a predictive model (a.k.a. metamodel) for real-time decision-making. For example, Hannah et al. (2010) used nonparametric density estimation to study a simulation optimization problem with covariates; Jiang et al. (2020) built a logistic regression model using offline simulation to monitor online risk; and Shen et al. (2021) employed linear models via simulation to study ranking and selection with covariates for personalized decision-making.

Metamodeling constitutes the core of the OSOA framework. Within this framework, during the offline stage, multiple simulation experiments are conducted with varying covariate values to collect a dataset $\{(\mathbf{x}_i, y_i)\}_{i=1}^n$. This data is then used to fit a metamodel for a specified summary statistic as a function of the covariates. For instance, Hannah et al. (2010) focused on the expected revenue that depends on the wind speed an hour later, Jiang et al. (2020) considered the probability of the portfolio loss beyond a threshold, and Shen et al. (2021) modeled the expected quality-adjusted life years of a patient under different treatments. Many metamodeling techniques have been proposed, including linear regression, kernel regression, radial basis functions, stochastic kriging, and neural networks; see Barton (2020) for an overview on simulation metamodeling. However, a major limitation of these traditional metamodeling techniques is the necessity to specify the summary statistics in advance. This may not be suitable for numerous practical real-time decision-making problems, where different summary statistics might be employed in different scenarios. For instance, in the area of personalized medicine, not all patients prioritize the expected number of life years; some may be more interested in the probability of survival beyond a certain critical time point.

However, this information only becomes available after the doctor’s consultation with the patient, that is, after the covariate values have been revealed.

A natural question arises: *what would be an ideal metamodel?* To answer this, let us consider a hypothetical scenario where a super-fast computer is at our disposal, capable of generating simulation observations instantaneously. In this scenario, there would be no need to construct a metamodel. Instead, one could simply wait until the covariate values are revealed, run the simulation model to generate as many output observations as needed, and then calculate any summary statistics of these simulation outputs using the observations. Of course, this is purely a hypothetical scenario, but it sheds light on the characteristics of an ideal metamodel. In our opinion, given the covariates, an ideal metamodel should generate random outputs that share the same distribution as the original simulator’s outputs, but at a much faster speed. This problem can be formulated as using the data $\{(\mathbf{x}_i, y_i)\}_{i=1}^n$ to construct a fast generative model $\hat{Y}(\mathbf{x})$ such that $\hat{Y}(\mathbf{x})$ matches $Y(\mathbf{x})$ in distribution, at least approximately. In other words, our goal is to build a “fast simulator of the simulator”, a concept we refer to as a *generative metamodel*. Once the covariate values are revealed, we can apply the generative metamodel to instantaneously generate a large number of observations. These observations can then be used to compute any summary statistics in real time.

The objective in constructing a generative metamodel is to learn the conditional distribution of the simulation output, given the covariates. This task bears a resemblance to generative modeling in the field of machine learning. A leading method of generative modeling in machine learning is the generative adversarial network (GAN). This technique involves two neural networks competing against each other to generate new data that mirrors a specific training dataset. The concept of GANs was initially proposed by Goodfellow et al. (2014), and has been extensively studied and diversified since its inception. In particular, the conditional GAN (CGAN), introduced by Mirza and Osindero (2014), allows the use of covariates for generating conditional samples. More recently, the diffusion model became a popular generative modeling method in machine learning. Proposed by Ho et al. (2020), this model generates high-quality data by reversing a forward diffusion process that progressively transforms the data into white noise. In addition to these two popular methods, there are other generative modeling techniques in machine learning, such as variational autoencoders (Kingma and Welling 2013), normalizing flows (Rezende and Mohamed 2015), and autoregressive generative models (Bengio et al. 2003). These methods have demonstrated remarkable results across numerous applications, particularly in the generation of images.

However, our problems generally possess distinct characteristics compared to the typical applications of generative models in machine learning:

- **Observation Replication:** Our primary concern lies in producing a large number of observations that well-replicate the real distribution, including the distribution tails. In contrast,

in machine learning, the goal is often to produce a few high-quality observations, such as realistic-looking images. It’s worth noting that many machine learning methods are known to struggle with mode collapse problems (Saxena and Cao 2021), meaning that the generated data do not have the diversity observed in the real data and do not replicate the real distribution.

- **Data-Generation Speed:** We want a generative metamodel with a high data-generation speed to facilitate real-time decision-making. Therefore, methods like diffusion models, which tend to have a slow generation speed because of the need for thousands of steps to generate an observation, are not suitable.
- **Covariate Nature:** In our applications, covariates are typically continuous variables, whereas machine learning often deals more with categorical labels. Although there are some studies on continuous labels, they are relatively rare.
- **Output Dimensionality:** Our focus is on cases where the output of the simulation model is one-dimensional or low-dimensional, corresponding to most practical simulation problems. In contrast, machine learning is more focused on higher-dimensional data, such as images, speech, and videos.

In this paper we consider only the one-dimensional case where the simulation output is a random variable, although the covariates are multi-dimensional, and leave the multi-dimensional case for future research. In the simulation literature, the most fundamental approach to generating observations from a random variable is the *inverse transform method*. It generates random observations by calculating the target distribution’s quantile specified at a random level that is uniformly distributed in $(0, 1)$. Therefore, the key to generative metamodeling lies in learning the inverse cumulative distribution function of Y given \mathbf{x} . This function is precisely the *conditional quantile function*, denoted as $F_Y^{-1}(\tau|\mathbf{x})$ for $\tau \in (0, 1)$. This insight motivates us to learn $F_Y^{-1}(\tau|\mathbf{x})$ at a grid of τ values applying quantile regression on the dataset $\{(\mathbf{x}_i, y_i)\}_{i=1}^n$, and to interpolate for τ values not present on the grid. Once the conditional quantile function is learned, it can be easily used to generate random observations after the covariates are observed. We refer to this method as quantile-regression-based generative metamodeling (QRGMM).

We study the asymptotic behaviors of QRGMM as the number of simulation observations approaches infinity. We prove that the distribution of the generated observations converge to the true conditional distribution under mild conditions. It’s important to underline that while the convergence analysis heavily depends on the asymptotic behaviors of quantile-regression estimators, the analysis conducted in this paper is significantly more complex from a technical viewpoint. This is because traditional quantile regression results are typically established for either a fixed $\tau \in (0, 1)$ or a range of values that are bounded away both from 0 and 1. In our analysis, it is critical to

handle the tails of the conditional distribution to ensure convergence, because the tails of a quantile function often explode to infinity rapidly as τ approaches 0 or 1; see Figure 1 in Section 4.

Apart from the convergence in distribution, we also investigate the rate of convergence, a topic complicated by the tail behaviors of the target conditional distribution. We first examine the rate of convergence of $\hat{Y}(\tau|\mathbf{x})$, which is the estimator of the conditional quantile function $F_Y^{-1}(\tau|\mathbf{x})$, for a given \mathbf{x} . We prove that its rate of convergence is $1/\sqrt{n} + 1/m$ when τ belongs to an open subset of $(0, 1)$, where n is the number of simulation observations and m is the number of grid points of τ . By incorporating extreme value theory, we also show that $\hat{Y}(\tau|\mathbf{x})$ does not have a universal rate of convergence when τ is near 0 or 1; instead, it depends on the tail behaviors of the conditional distribution of Y given \mathbf{x} . Nevertheless, we find that surprisingly, there does exist a uniform convergence—which is also at a rate of $1/\sqrt{n} + 1/m$ —for the distribution of the generative metamodel $\hat{Y}(\mathbf{x})$ (i.e., $\hat{Y}(U|\mathbf{x})$, where U is a uniform random variable).

The application of quantile regression in building generative models have also been explored in the machine-learning literature. Dabney et al. (2018a,b) were the first to generalize the deep Q-learning algorithm of Mnih et al. (2015), using quantile regression neural networks to build generative models of the value distribution in reinforcement learning. They proposed an implicit quantile networks (IQN) approach, which also incorporates the quantile level as an input. Further, Ostrovski et al. (2018) combined IQN with the chain rule of probability to propose PixelIQN for image generation, based on the PixelCNN architecture of van den Oord et al. (2016). Wen and Torkkola (2019) suggested an alternative method for learning the joint distribution by combining quantile regression with copulas. Recently, combined with recurrent neural networks, quantile function modeling has been applied to probabilistic time series forecasting (Gouttes et al. 2021) and predictive-model building for continuous-time event data under the framework of temporal point processes (Ben Taieb 2022). However, much of this research mainly focuses on the empirical performance of the generative models, with none providing any proven results on convergence or rate of convergence, which are crucial to simulation generative metamodeling.

The rest of the paper is organized as follows. Section 2 formulates the generative metamodeling problem, and Section 3 introduces QRGMM. The convergence-in-distribution of QRGMM is established in Section 4, followed by discussion on the rate of convergence in Section 5. A thorough numerical study is presented in Section 6. Section 7 concludes and the e-companion collects some technical proofs.

2. Problem Formulation

Suppose we have a simulator, denoted as ϕ . This simulator can be considered as a deterministic function without an analytical form, which maps the simulation input parameters \mathbf{x} and a random

vector ξ , which represents all the randomness inherent in the underlying system, to the simulation output $Y(\mathbf{x})$. This relationship can be expressed as:

$$Y(\mathbf{x}) = \phi(\mathbf{x}, \xi).$$

Here, $\mathbf{x} \in \mathcal{X} \subseteq \mathbb{R}^p$ is a p -dimensional vector, and it can be viewed as the covariates of the system. For example, in a Markovian queueing simulator, \mathbf{x} may include the arrival and service rates, while ξ corresponds to the sequence of exponential random variables used in the simulation. For a financial simulation predicting the future return of a portfolio, if the stock prices are modeled by a multi-dimensional geometric Brownian motion, \mathbf{x} may represent the weights of different financial instruments, and ξ may be the sequence of standard normal random variables simulating the Brownian motion. In a more general simulation context, ξ may be regarded as considered a set of uniform random variables that fundamentally drive the simulation. Throughout this paper, we assume that $Y(\mathbf{x})$ is one-dimensional, and we leave the discussion of multi-dimensional simulation outputs for future research.

In many practical applications, the simulator ϕ models a complex physical process, making it computationally demanding and time-consuming to run. To accelerate the use of simulation for real-time decision-making, metamodeling techniques are frequently employed. Suppose that there is a dataset $\{(\mathbf{x}_i, y_i)\}_{i=1}^n$ obtained through running independent simulation experiments at a sequence of covariate values $\mathbf{x}_1, \dots, \mathbf{x}_n$, where y_i is a random observation of $Y(\mathbf{x}_i)$. Classical metamodeling techniques use this dataset to build a metamodel of $\mu(\mathbf{x}) = \mathbb{E}[Y(\mathbf{x})]$ to capture the relationship between the expectation of $Y(\mathbf{x})$ and the covariate \mathbf{x} . Examples include linear regression, radial basis functions, stochastic kriging, among others; see, e.g., the review paper of Barton (2020). Other summary statistics of $Y(\mathbf{x})$ have also been considered in the metamodeling literature, including probabilities (Jiang et al. 2020) and quantiles (Chen and Kim 2016).

In this paper we propose a more flexible metamodeling concept called *generative metamodeling*. Instead of building a metamodel of a given summary statistic of $Y(\mathbf{x})$, we construct a metamodel of the random variable $Y(\mathbf{x})$. Our goal is to use the dataset $\{(\mathbf{x}_i, y_i)\}_{i=1}^n$ to construct a random function $\hat{Y}(\mathbf{x})$ that satisfies the following criteria:

- (i) $\hat{Y}(\mathbf{x})$ should have a distribution approximately identical to that of $Y(\mathbf{x})$ for any given $\mathbf{x} \in \mathcal{X}$.
- (ii) It should be possible to generate observations from $\hat{Y}(\mathbf{x})$ significantly faster than executing the simulation model $Y(\mathbf{x})$ for any given $\mathbf{x} \in \mathcal{X}$.

We call the random function $\hat{Y}(\mathbf{x})$ a generative metamodel, which can be seen as “a fast simulator of the simulator”. Notice that the generative metamodel is more flexible than traditional metamodels. With a traditional metamodel, given \mathbf{x} , one can only obtain a specific summary statistic of $Y(\mathbf{x})$,

such as $\mathbb{E}[Y(\mathbf{x})]$. In contrast, with a generative metamodel, given \mathbf{x} , one can quickly generate a sample of $\hat{Y}(\mathbf{x})$ and use this sample to approximate any summary statistics of $Y(\mathbf{x})$.

Before concluding this section, we make a remark concerning the dataset $\{(\mathbf{x}_i, y_i)\}_{i=1}^n$. It is well known that experimental design—that is, how to design a simulation experiment to acquire the dataset—is a crucial research issue that can improve the quality of the metamodel (Barton 2020). In this paper, however, we proceed under the premise that a dataset already exists. This dataset may have been collected through a well-planned experimental design or could simply be a record of past experiments. We focus on how to build a generative metamodel given this dataset, and leave the problem of experimental design for future research.

3. Quantile-Regression-based Generative Metamodeling

Despite existing generative methods in the field of machine learning, we must reiterate that our problems possess distinct characteristics from theirs. First, our focus is more on the similarity (from a distributional perspective) between the generative data and the original data, as well as the speed of generation. In contrast, machine learning problems place more emphasis on the quality of the generated instances such as images. Second, we focus on cases with continuous covariates \mathbf{x} and one-dimensional output $Y(\mathbf{x})$, whereas machine learning problems often involve categorical covariates and high-dimensional output.

3.1. Inverse Transform

A fundamental approach to random-variate generation from a simulation perspective is the inverse transform method (Banks et al. 2009). Suppose that a random variable Y has a distribution function $F(\cdot)$. Let $F^{-1}(\tau) = \inf\{y : F(y) \geq \tau\}$ for any $\tau \in (0, 1)$ be the quantile function of Y . It is known that $F^{-1}(U)$ has the same distribution as Y where U follows the uniform distribution in $(0, 1)$. Therefore, the inverse transform method generates random observations of Y by calculating $F^{-1}(U)$ with randomly generated U . Returning to our problem, we denote the quantile function of $Y(\mathbf{x})$ as $F_Y^{-1}(\tau|\mathbf{x})$, for $\tau \in (0, 1)$. If $F_Y^{-1}(\tau|\mathbf{x})$ is available for any $\tau \in (0, 1)$ and $\mathbf{x} \in \mathcal{X}$, we can then use the inverse transform method to easily generate $Y(\mathbf{x})$. However, it is not directly available. In this paper, we propose a quantile-regression-based approach to learn the (conditional) quantile function $F_Y^{-1}(\tau|\mathbf{x})$ using the dataset $\{(\mathbf{x}_i, y_i)\}_{i=1}^n$.

To model this conditional quantile function, we apply a linear quantile regression model $Q_\tau(\mathbf{x})$ at level τ . In this paper, we assume no model misspecification, that is, $Q_\tau(\mathbf{x}) = \beta(\tau)^\top \mathbf{x}$ is identical to $F_Y^{-1}(\tau|\mathbf{x})$. Alternative quantile regression models are also feasible for $Q_\tau(\mathbf{x})$, including neural networks, random forests, kriging, and many others; see the review paper of Torossian et al. (2020) and references therein. The only remaining question is how to handle τ , which varies over the range of $(0, 1)$, rather than being fixed.

One approach to handling the varying τ in the inverse transform method is to first sample a uniform random variable U , and then conduct a quantile regression to estimate $Q_U(\mathbf{x})$ with $\tau = U$. With the estimated $Q_U(\mathbf{x})$, we can then plug in the observed \mathbf{x} to generate an (approximate) observation of $Y(\mathbf{x})$. One problem with this approach is that it is computationally expensive. For each observation of $Y(\mathbf{x})$, a quantile-regression model needs to be fitted. When dealing with a large amount of data or when the fitting method is computationally expensive, this approach often proves too slow to support real-time decision making.

We propose another approach to handling the varying τ . First, we discretize $(0, 1)$ to a set of $m - 1$ equally-spaced values with $\tau_j = j/m, j = 1, \dots, m - 1$. We then apply a quantile regression model to fit the $m - 1$ quantile functions $Q_{\tau_j}(\mathbf{x}), j = 1, \dots, m - 1$ using the dataset $\{(\mathbf{x}_i, y_i)\}_{i=1}^n$ and denote them as $\hat{Q}_{\tau_j}(\mathbf{x}), j = 1, \dots, m - 1$. These fittings may be computationally expensive, but they are performed in the offline stage. Then, in the online stage, once the covariate \mathbf{x} is observed, we may generate a uniform random variable U and approximate $Q_U(\mathbf{x})$ by a linear interpolation scheme of $Q_{\tau_j}(\mathbf{x}), j = 1, \dots, m - 1$. This can be done quickly and is therefore suitable for real-time decision-making.

Based on the approach, we propose QRGMM as shown in Algorithm 1. Notice that the goal of this algorithm is to instantaneously generate a set of K approximate observations of $Y(\mathbf{x}^*)$, denoted by $\hat{Y}_1(\mathbf{x}^*), \dots, \hat{Y}_K(\mathbf{x}^*)$, once we observe that the covariates $\mathbf{x} = \mathbf{x}^*$. Then, we can use the observations to estimate any summary statistics of $Y(\mathbf{x}^*)$.

Algorithm 1 QRGMM

Offline Stage:

- Collect the dataset $\{(\mathbf{x}_i, y_i)\}_{i=1}^n$.
- Choose a positive integer m , and discretize $[0, 1]$ by $\tau_j = \frac{j}{m}, j = 1, 2, \dots, m - 1$.
- Fit the quantile regression model $\hat{Q}_{\tau_j}(\mathbf{x})$ with the dataset for all $j = 1, \dots, m - 1$.

Online Stage:

- Observe the covariate $\mathbf{x} = \mathbf{x}^*$.
- Generate u_1, \dots, u_K independently from the uniform distribution in $(0, 1)$.
- For $k = 1, 2, \dots, K$, output

$$\hat{Y}_k(\mathbf{x}^*) = \begin{cases} \hat{Q}_{\tau_1}(\mathbf{x}^*), & u_k < \tau_1, \\ \hat{Q}_{\tau_j}(\mathbf{x}^*) + m(u_k - \tau_j) \left[\hat{Q}_{\tau_{j+1}}(\mathbf{x}^*) - \hat{Q}_{\tau_j}(\mathbf{x}^*) \right], & u_k \in [\tau_j, \tau_{j+1}), j = 1, 2, \dots, m - 2, \\ \hat{Q}_{\tau_{m-1}}(\mathbf{x}^*), & u_k \geq \tau_{m-1}. \end{cases}$$

Notice that when generating random observations, the tail behaviors (i.e., as τ approaches 0 or 1) of the random variable $Y(\mathbf{x})$ are generally difficult to capture. In QRGMM, we introduce

the parameter m not only to control the learning fidelity, but also to provide a way to handle the tails. As m increases, the endpoints of the quantile levels approach 0 and 1. As such, it is critical to understand how m should depend on the data size n to ensure the convergence (e.g., the convergence in distribution). This is an important issue to consider in Sections 4 and 5.

3.2. Linear Quantile Regression Model

Throughout the rest of the paper, we assume the simulation output $Y(\mathbf{x})$ is a continuous random variable on its support given the input \mathbf{x} . We denote the conditional distribution and density functions as $F_Y(\cdot|\mathbf{x})$ and $f_Y(\cdot|\mathbf{x})$, respectively. Furthermore, we impose the following assumption on the conditional quantile function.

ASSUMPTION 1. $F_Y^{-1}(\tau|\mathbf{x}) = \boldsymbol{\beta}(\tau)^\top \mathbf{x}$ all $\tau \in (0, 1)$ and $\boldsymbol{\beta}(\tau)$ is continuous in τ .

Assumption 1 basically assumes that the linear quantile regression model is the true model of the conditional quantile functions of Y given \mathbf{x} on $\tau \in (0, 1)$, i.e., $F_Y^{-1}(\tau|\mathbf{x})$ is linear in covariates \mathbf{x} for any $\tau \in (0, 1)$. We need this assumption to understand the convergence behaviors of the proposed QRGMM algorithm, though any quantile regression models may be used in the algorithm. An important special case of Assumption 1 is the *location-scale shift* model, i.e.,

$$Y(\mathbf{x}) = \boldsymbol{\alpha}^\top \mathbf{x} + (\boldsymbol{\gamma}^\top \mathbf{x})\varepsilon,$$

where ε is a univariate random error whose distribution is F_0 and it determines the shape of the distribution of $Y(\mathbf{x})$. Then, it is easy to see that

$$F_Y^{-1}(\tau|\mathbf{x}) = \boldsymbol{\alpha}^\top \mathbf{x} + \boldsymbol{\gamma}^\top \mathbf{x} F_0^{-1}(\tau), \quad \tau \in (0, 1)$$

where $F_0^{-1}(\tau)$ is the τ -quantile of ε . Notice that, under the location-scale shift model, Assumption 1 does not make any distribution assumption on ε . This is the well-known distribution-free property of quantile regression (Koenker 2005).

Although Assumption 1 may seem restrictive, it is widely used in practice due to its simplicity and interpretability. Besides, combined with domain knowledge, it can be extended to capture nonlinearity by substituting \mathbf{x} by a set of nonlinear basis functions $\mathbf{b}(\mathbf{x})$ of \mathbf{x} . As for the theoretical analysis, we use \mathbf{x} throughout the paper for convenience, but the results can be easily extended when basis functions are used. Moreover, our numerical experiments show that even in cases where the linear quantile regression model assumption is not valid, this approximation may still yield favorable outcomes.

Given Assumption 1, using the dataset $\{(\mathbf{x}_i, y_i)\}_{i=1}^n$, for any fixed $\tau \in (0, 1)$, we may estimate $\boldsymbol{\beta}(\tau)$ by

$$\hat{\boldsymbol{\beta}}(\tau) = \operatorname{argmin}_{\boldsymbol{\beta} \in \mathbb{R}^p} \sum_{i=1}^n \rho_\tau(y_i - \boldsymbol{\beta}^\top \mathbf{x}_i), \quad (1)$$

where $\rho_\tau(u) = [\tau - I(u \leq 0)]u$ is the pinball loss function (Koenker 2005). Problem (1) may be reformulated as a linear program and, thus, can be solved efficiently even when n is large (Koenker 2017), and the statistical properties of $\hat{\beta}(\tau)$ are well studied in the literature (Koenker 2005).

Once we obtain the $\hat{\beta}(\tau)$, we may estimate the τ -quantile function $Q_\tau(\mathbf{x})$ by $\hat{Q}_\tau(\mathbf{x}) = \hat{\beta}(\tau)^\top \mathbf{x}$ and use it in QRGMM. More specifically, in the offline stage of algorithm, we estimate the coefficients of the quantile functions at a predetermined set $\{\tau_j = \frac{j}{m}, j = 1, 2, \dots, m-1\}$ using the linear quantile regression model such that

$$\hat{\beta}(\tau_j) = \underset{\beta}{\operatorname{argmin}} \sum_{i=1}^n \rho_{\tau_j}(y_i - \beta^\top \mathbf{x}_i), \quad j = 1, 2, \dots, m-1.$$

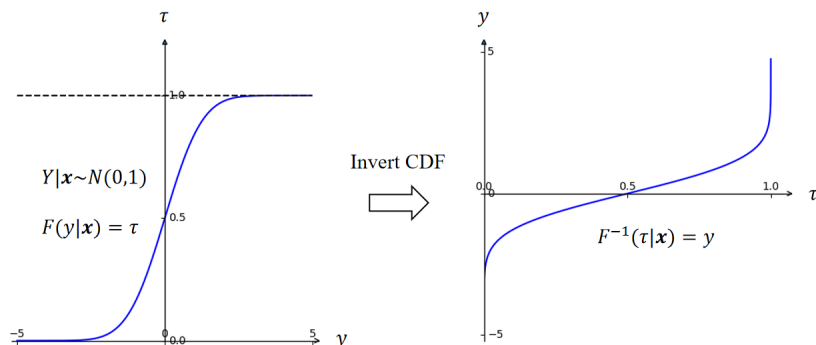
We can then obtain $\hat{Q}_{\tau_j}(\mathbf{x}) = \hat{\beta}(\tau_j)^\top \mathbf{x}$ for all $j = 1, \dots, m-1$ and use them in QRGMM.

4. Convergence in Distribution

In this section we establish the convergence in distribution of the observations generated by QRGMM. In particular, we want to show that $\hat{Y}(\mathbf{x}^*)$ converges in distribution to $Y(\mathbf{x}^*)$ as the data size n goes to infinity for any fixed $\mathbf{x}^* \in \mathcal{X}$. As we point out in the introduction, in simulation generative metamodeling, we want to generate random observations that replicate the distribution of the simulation output given the value of the covariates. Therefore, the convergence in distribution provides a reassurance that the proposed algorithm is valid in achieving the goal.

However, establishing the convergence in distribution is not trivial. Notice that we may write $Y(\mathbf{x}^*) = F_Y^{-1}(U|\mathbf{x}^*)$ where U follows the uniform distribution in $(0, 1)$. As shown in Figure 1, the conditional quantile function $F_Y^{-1}(\tau|\mathbf{x}^*)$ may go to infinity very quickly as τ approaches 0 or 1 if Y has an infinity support. Thus, to establish the convergence in distribution, a generative-metamodeling algorithm needs to carefully consider the handling of the tails and bound the approximation errors, which is also the key in our analysis of the convergence of QRGMM in distribution .

Figure 1 Cumulative Distribution Function and Quantile Function of $Y(\mathbf{x})$.



4.1. Preliminaries

In this subsection, we first present some preliminary results for establishing the convergence of QRGMM in distribution. Beyond Assumption 1, we require the following two assumptions.

ASSUMPTION 2. (2.a) *The distribution $F_Y(\cdot|\mathbf{x})$ is absolutely continuous on a common support for all $\mathbf{x} \in \mathcal{X}$.*

(2.b) *For any given interval $[\tau_\ell, \tau_u] \subset (0, 1)$ with $0 < \tau_\ell < \tau_u < 1$, the density functions $f_Y(\cdot|\mathbf{x})$ are uniformly bounded away from 0 and ∞ in the sense that*

$$0 < \inf_{\tau \in [\tau_\ell, \tau_u]} \inf_{\mathbf{x} \in \mathcal{X}} f_Y(F_Y^{-1}(\tau|\mathbf{x})|\mathbf{x}) \leq \sup_{\tau \in [\tau_\ell, \tau_u]} \sup_{\mathbf{x} \in \mathcal{X}} f_Y(F_Y^{-1}(\tau|\mathbf{x})|\mathbf{x}) < \infty.$$

ASSUMPTION 3. (3.a) *For any given interval $[\tau_\ell, \tau_u] \subset (0, 1)$ with $0 < \tau_\ell < \tau_u < 1$, there exist positive definite matrices D_0 and $D_1(\tau)$ such that*

$$\lim_{n \rightarrow \infty} \frac{1}{n} \sum_{i=1}^n \mathbf{x}_i \mathbf{x}_i^\top = D_0 \quad \text{and} \quad \lim_{n \rightarrow \infty} \frac{1}{n} \sum_{i=1}^n f_Y(F_Y^{-1}(\tau|\mathbf{x}_i)|\mathbf{x}_i) \mathbf{x}_i \mathbf{x}_i^\top = D_1(\tau)$$

uniformly for $\tau \in [\tau_\ell, \tau_u]$.

(3.b) $\max_{1 \leq i \leq n} \|\mathbf{x}_i\| = o(\sqrt{n})$.

Assumption 2 is on the distribution of $Y(\mathbf{x})$. Assumption (2.a) is an elemental smoothness condition, commonly assumed for distribution functions. Assumption (2.b) requires that the density function of $Y(\mathbf{x})$, i.e., $f_Y(\cdot|\mathbf{x})$, are uniformly bounded away from 0 and ∞ on the interval defined by the τ_ℓ and τ_u quantiles of $Y(\mathbf{x})$, where one may notice that $F_Y^{-1}(\tau|\mathbf{x})$ is the τ -quantile of $Y(\mathbf{x})$. Both Assumptions (2.a) and (2.b) can be easily satisfied, especially when the covariate set \mathcal{X} is bounded.

Assumption 3 is on the property of the design points (i.e., observed covariates in the dataset) $\mathbf{x}_1, \dots, \mathbf{x}_n$. Notice that when the covariate set \mathcal{X} is bounded, both Assumptions (3.a) and (3.b) hold. Assumptions 2 and 3 are both commonly used assumptions in the literature of quantile regression. For more details on these two assumptions, see Section 4 of Koenker (2005).

In addition to the commonly used $o(\cdot)$ and $O(\cdot)$ notation, we also employ their stochastic counterparts in this paper, denoted as $o_{\mathbb{P}}(\cdot)$ and $O_{\mathbb{P}}(\cdot)$, respectively, which are frequently used in statistics literature. Specifically, $o_{\mathbb{P}}(1)$ represents a sequence of random vectors that converges to zero in probability, while the notation $O_{\mathbb{P}}(1)$ denotes a sequence of random variables that are bounded in probability. Similar to $o(r_n)$ and $O(r_n)$, the expressions $o_{\mathbb{P}}(r_n)$ and $O_{\mathbb{P}}(r_n)$ can be understood as the sequences they represented divided by r_n following the meaning of $o_{\mathbb{P}}(1)$ and $O_{\mathbb{P}}(1)$. For more details on the notation, please refer to Section 2.2 of Van der Vaart (2000).

To establish the convergence of QRGMM in distribution, we also need two preliminary lemmas. The first one is the Bahadur representation of the coefficient estimator $\hat{\beta}(\tau)$ of the quantile regression.

LEMMA 1 (**Bahadur Representation, Koenker (2005)**). *For any given interval $[\tau_\ell, \tau_u] \subset (0, 1)$ with $0 < \tau_\ell < \tau_u < 1$, denote $\hat{\beta}(\tau)$ as the estimator of $\beta(\tau)$ via the quantile regression method for $\tau \in [\tau_\ell, \tau_u]$. Under Assumptions 1–3, $\sqrt{n} \left[\hat{\beta}(\tau) - \beta(\tau) \right]$, as a stochastic process on $[\tau_\ell, \tau_u]$, admits the following Bahadur representation*

$$\sqrt{n} \left[\hat{\beta}(\tau) - \beta(\tau) \right] = D_1^{-1}(\tau) W_n(\tau) + o_{\mathbb{P}}(1), \quad (2)$$

as $n \rightarrow \infty$, uniformly over $\tau \in [\tau_\ell, \tau_u]$. Here,

$$W_n(\tau) = \frac{1}{\sqrt{n}} \sum_{i=1}^n \mathbf{x}_i \psi_\tau(y_i - \beta(\tau)^\top \mathbf{x}_i) \Rightarrow N(0, \tau(1-\tau)D_0),$$

as $n \rightarrow \infty$, where $\psi_\tau(u) = \tau - \mathbb{I}\{u \leq 0\}$, “ \Rightarrow ” denotes convergence in distribution, and $N(\mu, \sigma^2)$ denotes a normal distribution with mean μ and variance σ^2 . Moreover, as described in Section 4.3 of Koenker (2005), there exists a p -dimensional standard Brownian bridge \mathbf{B} on $[0, 1]$ such that

$$\sqrt{n} D_0^{-1/2} D_1(\tau) \left[\hat{\beta}(\tau) - \beta(\tau) \right] \Rightarrow \mathbf{B}(\tau), \quad (3)$$

as $n \rightarrow \infty$, uniformly over $\tau \in [\tau_\ell, \tau_u]$.

Notice that the Bahadur representation was originally developed for quantile estimation (Bahadur 1966) and it played a critical role in understanding the asymptotic behaviors of many quantile estimators, e.g., the importance-sampling quantile estimators of Sun and Hong (2010) and Chu and Nakayama (2012). Lemma 1 extends the result to quantile regression not only for a fixed $\tau \in [\tau_\ell, \tau_u]$ value but also for the entire interval $[\tau_\ell, \tau_u]$. Therefore, Equation (2) is an asymptotic representation of a stochastic process defined on $[\tau_\ell, \tau_u]$ instead of that of a random variable with a fixed τ . With the asymptotic representation, Lemma 1 shows that the stochastic process converges in distribution to a Brownian bridge in Equation (3), which is a very interesting result. This result is critical to our analysis, because we are also interested in the convergence behavior of the entire function $F_Y^{-1}(\tau|\mathbf{x})$ for $\tau \in (0, 1)$ instead of a fixed τ .

By Assumptions (2.b) and (3.a), we have $\sup_{\tau \in [\tau_\ell, \tau_u]} \|D_1^{-1}(\tau)\| < \infty$. Hence, by Equation (3) of Lemma 1, it is easy to derive the uniform convergence of $\hat{\beta}(\tau_j)$ on $[\tau_\ell, \tau_u]$, which is shown in the following Proposition 1.

PROPOSITION 1. *Under Assumptions 1–3, for any given interval $[\tau_\ell, \tau_u]$ with $0 < \tau_\ell < \tau_u < 1$,*

$$\max_{\substack{\tau_j \in [\tau_\ell, \tau_u] \\ 1 \leq j \leq m-1}} \left\| \hat{\beta}(\tau_j) - \beta(\tau_j) \right\| \xrightarrow{\mathbb{P}} 0$$

as $n \rightarrow \infty$, where $\tau_j = \frac{j}{m}$ for $j = 1, \dots, m$.

Notice that Lemma 1 and Proposition 1 only provide convergence results for the coefficients of quantile regression on any given interval $[\tau_\ell, \tau_u]$. It is not sufficient for the convergence of $\hat{Y}(\mathbf{x}^*)$ in distribution, generated using QRGMM, because some τ_j 's will not be in a fixed interval $[\tau_\ell, \tau_u]$ as $m \rightarrow \infty$. Therefore, how to handle the tail behaviors remains a challenge.

The second preliminary lemma that we need to establish the convergence of QRGMM in distribution is the Portmanteau lemma, which is commonly used in proving convergence in distribution.

LEMMA 2 (Portmanteau Lemma, Lemma 2.2 in Van der Vaart (2000)). *The following two statements are equivalent for any random vectors X_n and X :*

(i) $X_n \Rightarrow X$ as $n \rightarrow \infty$;

(ii) $\mathbb{E}[h(X_n)] \rightarrow \mathbb{E}[h(X)]$ as $n \rightarrow \infty$ for all bounded Lipschitz continuous functions $h(\cdot)$.

The Portmanteau lemma shows that, to establish the convergence of X_n to X in distribution, it is equivalent to prove the convergence of $\mathbb{E}[h(X_n)]$ to $\mathbb{E}[h(X)]$ for any bounded Lipschitz continuous function $h(\cdot)$. It allows a better way to handle the tails of X_n because, while the tails of X_n may be unbounded and may grow to infinity very quickly, the tails of $h(X_n)$ are bounded and its growth rate is bounded by the Lipschitz constant, which is critical in the proving of the convergence of QRGMM in distribution .

4.2. Establishing the Convergence in Distribution

In this subsection our goal is prove $\hat{Y}(\mathbf{x}^*) \Rightarrow Y(\mathbf{x}^*)$ as $n \rightarrow \infty$ for any fixed $\mathbf{x}^* \in \mathcal{X}$. Let $\hat{Y}(U|\mathbf{x}) = \hat{Y}(\mathbf{x})$ to emphasize the role of the Uniform(0, 1) random variable U in the generation of $\hat{Y}(\mathbf{x})$. Furthermore, notice that $Y(\mathbf{x}) = F_Y^{-1}(U|\mathbf{x})$. Then, proving the convergence in distribution is equivalent to proving $\hat{Y}(U|\mathbf{x}^*) \Rightarrow F_Y^{-1}(U|\mathbf{x}^*)$, which by the Portmanteau lemma is equivalent to proving that

$$\mathbb{E} \left[h \left(\hat{Y}(U|\mathbf{x}^*) \right) \right] \rightarrow \mathbb{E} \left[h \left(F_Y^{-1}(U|\mathbf{x}^*) \right) \right] \quad \text{as } n \rightarrow \infty \quad (4)$$

for any given bounded Lipschitz continuous functions h . Notice that Equation (4) is not only an equivalent form of the convergence in distribution that we try to establish, it is often the goal of generative metamodeling. In generative metamodeling, we are often interested in generating observations to estimate the expectation of a performance function of the simulation output, which is in the form of the right-hand side of Equation (4).

Let M_h denote the bound and L_h denote the Lipschitz constant of such that $|h(y)| \leq M_h$ for all $y \in \mathcal{Y}$ and $|h(y_1) - h(y_2)| \leq L_h|y_1 - y_2|$ for all $y_1, y_2 \in \mathcal{Y}$. For any $\varepsilon > 0$, we let

$$\tau_\ell = \frac{\varepsilon}{10 \max(M_h, 1)} \quad \text{and} \quad \tau_u = 1 - \frac{\varepsilon}{10 \max(M_h, 1)}. \quad (5)$$

As the Uniform(0, 1) random variable U is in the range (0, 1), we break (0, 1) into the following 5 disjoint intervals,

$$I_1 = (0, \tau_\ell), I_2 = \left[\tau_\ell, \tau_\ell + \frac{1}{m} \right), I_3 = \left[\tau_\ell + \frac{1}{m}, \tau_u - \frac{1}{m} \right], I_4 = \left(\tau_u - \frac{1}{m}, \tau_u \right], I_5 = (\tau_u, 1). \quad (6)$$

To prove Equation (4), we prove that

$$\mathbb{E} \left[\left| h \left(\hat{Y}(U|\mathbf{x}^*) \right) - h \left(F_Y^{-1}(U|\mathbf{x}^*) \right) \right| \cdot \mathbb{I}\{U \in I_i\} \right] \leq \frac{\varepsilon}{5} \quad (7)$$

for all $i = 1, \dots, 5$. For the 5 disjoint intervals, I_1 and I_5 are the tails, and I_3 is the middle interval. Notice that I_3 is a subset of $[\tau_\ell, \tau_u] \cap \left[\frac{1}{m}, 1 - \frac{1}{m} \right]$. We define it in this way is to ensure that I_3 is within $[\tau_1, \tau_{m-1}]$, where QRGMM has explicit control on the accuracy. The intervals I_2 and I_4 are for technical completeness and they may be viewed as parts of the tails.

We first prove the following lemma on the tail intervals, i.e., I_1, I_2, I_4 and I_5 .

LEMMA 3. *For any bounded Lipschitz continuous function h and $\varepsilon > 0$, let τ_ℓ and τ_u be the ones defined by Equation (5), and I_1, I_2, I_4 and I_5 be the ones defined by Equation (6). Then, for large enough m , we have*

$$\mathbb{E} \left[\left| h \left(\hat{Y}(U|\mathbf{x}^*) \right) - h \left(F_Y^{-1}(U|\mathbf{x}^*) \right) \right| \cdot \mathbb{I}\{U \in I_i\} \right] \leq \frac{\varepsilon}{5}$$

for all $i = 1, 2, 4, 5$ and for any $\mathbf{x}^* \in \mathcal{X}$.

Proof. For $i = 1, 5$, we have

$$\mathbb{E} \left[\left| h \left(\hat{Y}(U|\mathbf{x}^*) \right) - h \left(F_Y^{-1}(U|\mathbf{x}^*) \right) \right| \cdot \mathbb{I}\{U \in I_i\} \right] \leq 2M_h \cdot \Pr\{U \in I_i\} = \frac{2M_h \cdot \varepsilon}{10 \max(M_h, 1)} \leq \frac{\varepsilon}{5}.$$

For $i = 2, 4$, we have

$$\mathbb{E} \left[\left| h \left(\hat{Y}(U|\mathbf{x}^*) \right) - h \left(F_Y^{-1}(U|\mathbf{x}^*) \right) \right| \cdot \mathbb{I}\{U \in I_i\} \right] \leq 2M_h \cdot \Pr\{U \in I_i\} = \frac{2M_h}{m} \leq \frac{\varepsilon}{5},$$

when $m \geq 10 \max(M_h, 1)/\varepsilon$. \square

REMARK 1. Lemma 3 shows that the tail errors of QRGMM may be controlled and it will not affect the convergence in distribution. Even though the proof of the lemma appears trivial, it shows the importance of the Portmanteau lemma. As we mentioned earlier, the quantile function $F_Y^{-1}(\tau|\mathbf{x}^*)$ may go to infinity very quickly as τ approaches 0 or 1, if $Y(\mathbf{x}^*)$ has an infinite support. As a result, some of the sample paths of the tails may not converge of $\hat{Y}(\mathbf{x}^*)$. Therefore, it may not be possible to establish sample-path convergence, i.e., almost-sure convergence or strong convergence. However, the Portmanteau lemma bypasses the difficulty of directly handling the convergence for the tails of $\hat{Y}(\mathbf{x}^*)$. Instead, it looks at the tails of $h \left(\hat{Y}(\mathbf{x}^*) \right)$, which are bounded and whose errors are easier to control. In Section 5, we will study more complex behaviors of the tail convergence.

Next we analyze the middle interval $I_3 = [\tau_\ell + \frac{1}{m}, \tau_u - \frac{1}{m}]$. Notice that, in Remark 1, we mention that it may not be possible to establish sample-path convergence for the tails. For the middle interval, however, we are able to establish the following proposition on the uniform convergence of $\hat{Y}(\tau|\mathbf{x}^*)$ to $F_Y^{-1}(\tau|\mathbf{x}^*)$ on I_3 . The proof of the proposition is quite lengthy and we include it in the e-companion.

PROPOSITION 2. *Suppose that Assumptions 1–3 hold. Then, for any given $\mathbf{x}^* \in \mathcal{X}$, we have*

$$\begin{aligned} & \sup_{\tau \in I_3} \left| \hat{Y}(\tau|\mathbf{x}^*) - F_Y^{-1}(\tau|\mathbf{x}^*) \right| \\ & \leq \max_{\substack{\tau_j \in [\tau_\ell, \tau_u] \\ 1 \leq j \leq m-1}} \|\hat{\beta}_j - \beta(\tau_j)\| \cdot \|\mathbf{x}^*\| + \frac{1}{m} \left(\inf_{\tau \in [\tau_\ell, \tau_u]} f_Y(F_Y^{-1}(\tau|\mathbf{x}^*)|\mathbf{x}^*) \right)^{-1}. \end{aligned} \quad (8)$$

Furthermore, as $n, m \rightarrow \infty$,

$$\sup_{\tau \in I_3} \left| \hat{Y}(\tau|\mathbf{x}^*) - F_Y^{-1}(\tau|\mathbf{x}^*) \right| \xrightarrow{\mathbb{P}} 0.$$

Proposition 2 states that Assumptions 1–3 are sufficient for the uniform convergence of $\hat{Y}(\tau|\mathbf{x})$ on I_3 . Furthermore, by Equation (8), it is clear that the error of $\hat{Y}(\tau|\mathbf{x})$ can be bounded by the *estimation error* (i.e., the first term on the right-hand of the equation) and the *interpolation error* (i.e., the second term). By Proposition 1, the estimation error goes to zero as $n \rightarrow \infty$, and by Assumption (2.b), the interpolation error goes to zero as $m \rightarrow \infty$. We can then prove the following lemma that shows Equation (7) holds for I_3 as well.

LEMMA 4. *Suppose that Assumptions 1–3 hold. Then, for sufficiently large m and n ,*

$$\mathbb{E} \left[\left| h\left(\hat{Y}(U|\mathbf{x}^*)\right) - h\left(F_Y^{-1}(U|\mathbf{x}^*)\right) \right| \cdot \mathbb{I}\{U \in I_3\} \right] \leq \frac{\varepsilon}{5}$$

for any given $\mathbf{x}^* \in \mathcal{X}$.

Proof. For $I_3 = [\tau_\ell + \frac{1}{m}, \tau_u - \frac{1}{m}]$, notice that $h(\cdot)$ is a Lipschitz continuous function with the Lipschitz constant L_h , we have

$$\left| h\left(\hat{Y}(U|\mathbf{x}^*)\right) - h\left(F_Y^{-1}(U|\mathbf{x}^*)\right) \right| \cdot \mathbb{I}\{U \in I_3\} \leq L_h \cdot \sup_{\tau \in I_3} \left| \hat{Y}(\tau|\mathbf{x}^*) - F_Y^{-1}(\tau|\mathbf{x}^*) \right|.$$

By Proposition 2, for any given $\mathbf{x}^* \in \mathcal{X}$, as $n, m \rightarrow \infty$,

$$\sup_{\tau \in I_3} \left| \hat{Y}(\tau|\mathbf{x}^*) - F_Y^{-1}(\tau|\mathbf{x}^*) \right| \xrightarrow{\mathbb{P}} 0.$$

Then, we have

$$\left| h\left(\hat{Y}(U|\mathbf{x}^*)\right) - h\left(F_Y^{-1}(U|\mathbf{x}^*)\right) \right| \cdot \mathbb{I}\{U \in I_3\} \xrightarrow{\mathbb{P}} 0. \quad (9)$$

Moreover, since $h(\cdot)$ is bounded, we have that

$$\left| h\left(\hat{Y}(U|\mathbf{x}^*)\right) - h\left(F_Y^{-1}(U|\mathbf{x}^*)\right) \right| \cdot \mathbb{I}\{U \in I_3\} \leq 2M_h. \quad (10)$$

Then, by (9), (10), and the dominated convergence theorem (Van der Vaart 2000), we have

$$\mathbb{E} \left[\left| h \left(\hat{Y}(U|\mathbf{x}^*) \right) - h \left(F_Y^{-1}(U|\mathbf{x}^*) \right) \right| \cdot \mathbb{I}\{U \in I_3\} \right] \rightarrow 0$$

as $m, n \rightarrow \infty$. Therefore, for a given $\varepsilon > 0$, there exist sufficiently large M and N , such that for any $m \geq M$, $n \geq N$, we have that

$$\mathbb{E} \left[\left| h \left(\hat{Y}(U|\mathbf{x}^*) \right) - h \left(F_Y^{-1}(U|\mathbf{x}^*) \right) \right| \cdot \mathbb{I}\{U \in I_3\} \right] \leq \frac{\varepsilon}{5}.$$

This concludes the proof of the lemma. \square

Finally, by combining Lemmas 3 and 4 together, we have the following theorem on the convergence of $\hat{Y}(\mathbf{x}^*)$ in distribution. The more rigorous proof of the theorem is included in the e-companion.

THEOREM 1. *Under Assumptions 1–3, $\hat{Y}(\mathbf{x}^*) \rightarrow Y(\mathbf{x}^*)$ in distribution as $n, m \rightarrow \infty$ for any $\mathbf{x}^* \in \mathcal{X}$.*

The convergence in distribution established by Theorem 1 provides us valuable insights into the practical performance of QRGMM. When m and n are sufficiently large, the tails are well controlled even though there are no sample-path convergence. If we use the observations generated by QRGMM to evaluate an expectation of a performance function of $Y(\mathbf{x}^*)$, which is a very common task in simulation, as long as the dominated convergence theorem (Van der Vaart 2000) may be applied, the convergence in distribution also directly lead to the convergence in the expectation.

Theorem 1 also leads to the following corollary, which establishes the uniform convergence of the cumulative distribution function of $\hat{Y}(\mathbf{x}^*)$ to that of $Y(\mathbf{x}^*)$.

COROLLARY 1. *Under Assumptions 1–3,*

$$\sup_{y \in (-\infty, \infty)} |F_{\hat{Y}}(y|\mathbf{x}^*) - F_Y(y|\mathbf{x}^*)| \xrightarrow{\mathbb{P}} 0,$$

as $n, m \rightarrow \infty$ and for any $\mathbf{x}^* \in \mathcal{X}$, where $F_{\hat{Y}}(y|\mathbf{x}^*)$ is the cumulative distribution function of $\hat{Y}(\mathbf{x}^*)$.

Corollary 1 can be readily derived from Theorem 1 and Assumption (2.a), as the convergence in distribution and the continuity of the limit imply uniform convergence of the cumulative distribution function (Parzen 1960, Section 10.5).

5. Discussion on the Rate of Convergence

Section 4 shows that the observations generated by QRGMM converges in distribution to the true distribution. Consequently, a natural question arises: “*What is the rate of convergence?*” However, answering this question is significantly more difficult. Firstly, as discussed previously, the quantile function $F_Y^{-1}(\tau|\mathbf{x}^*)$ may rapidly approach infinity as τ approaches 0 or 1. Therefore, the middle

interval and the tails of the distributions may exhibit different rates of convergence. Secondly, the convergence in distribution proved in Section 4 does not imply the sample-path convergence of the random variables. As a result, if we only consider the tails, they may not converge at all.

In this section, we have three major results. In Section 5.1, we show that for a given \mathbf{x}^* , $\hat{Y}(\tau|\mathbf{x}^*)$, which is the estimator of $F_Y^{-1}(\tau|\mathbf{x}^*)$, converges at a rate of $1/\sqrt{n} + 1/m$, when τ lies in the middle interval. In Section 5.2, based on extreme value theory, we show that $\hat{Y}(\tau|\mathbf{x}^*)$ may not even converge when τ lies in the tail intervals, depending on the tail behaviors of the conditional distribution. In Section 5.3, somewhat surprisingly, we show in Corollary 1 that the distribution of $\hat{Y}(\mathbf{x}) = \hat{Y}(U|\mathbf{x}^*)$ admits a uniform convergence at a rate of $1/\sqrt{n} + 1/m$.

5.1. Rate of Convergence for the Middle Interval

In this subsection we examine the rate of convergence of $\hat{Y}(\tau|\mathbf{x}^*)$ in the middle interval, i.e., I_3 in Equation (6). From a data generation perspective, this subsection is crucial for many practical applications. We begin by explicitly deriving the rate of convergence of $\hat{\beta}_j$ within $[\tau_\ell, \tau_u]$, as stated in the following proposition.

PROPOSITION 3. *Under Assumptions 1–3, we have that as $n \rightarrow \infty$,*

$$\max_{\substack{\tau_j \in [\tau_\ell, \tau_u] \\ 1 \leq j \leq m-1}} \left\| \hat{\beta}_j - \beta(\tau_j) \right\| = O_{\mathbb{P}} \left(\frac{1}{\sqrt{n}} \right).$$

Proof. By Lemma 1, there exists a p -dimensional standard Brownian bridge \mathbf{B} on $[0, 1]$ such that uniformly for $\tau \in [\tau_\ell, \tau_u]$,

$$\sqrt{n} D_0^{-1/2} D_1(\tau) \left[\hat{\beta}(\tau) - \beta(\tau) \right] \Rightarrow \mathbf{B}(\tau).$$

This implies that

$$\sqrt{n} D_0^{-1/2} D_1(\tau_j) \left[\hat{\beta}_j - \beta(\tau_j) \right] = O_{\mathbb{P}}(1)$$

uniformly for all $\tau_j \in [\tau_\ell, \tau_u], j = 1, \dots, m$. Thus, by Assumptions (2.b) and (3.a), we have $\sup_{\tau \in [\tau_\ell, \tau_u]} \|D_1^{-1}(\tau)\| < \infty$, which implies

$$\max_{\substack{\tau_j \in [\tau_\ell, \tau_u] \\ 1 \leq j \leq m-1}} \sqrt{n} \left\| \hat{\beta}_j - \beta(\tau_j) \right\| = O_{\mathbb{P}}(1).$$

This concludes the proof of the proposition. \square

Then, combined with Proposition 2, the rate of convergence of $\hat{Y}(\tau|\mathbf{x}^*)$ for the middle interval can be easily obtained. We summarize the result in the following proposition.

PROPOSITION 4. *Under Assumptions 1–3, for any given \mathbf{x}^* , as $n, m \rightarrow \infty$,*

$$\sup_{\tau \in [\tau_\ell + \frac{1}{m}, \tau_u - \frac{1}{m}]} \left| \hat{Y}(\tau|\mathbf{x}^*) - F_Y^{-1}(\tau|\mathbf{x}^*) \right| = O_{\mathbb{P}} \left(\frac{1}{\sqrt{n}} \right) + O \left(\frac{1}{m} \right).$$

Proposition 4 indicates that the rate of convergence of $\hat{Y}(\tau|\mathbf{x}^*)$ generated by QRGM in the middle interval is determined by the slower rate between $1/\sqrt{n}$ and $1/m$. This result implies that m should grow at least at a rate of \sqrt{n} , so that the interpolation error does not dominate the estimation error. A practical guidance for selecting an appropriate value for m is to let $m = O(\sqrt{n})$, e.g., $m = \sqrt{n}$, to achieve the $1/\sqrt{n}$ rate of convergence while limiting the computational effort of fitting m quantile regression models.

5.2. Rate of Convergence for the Tails

The rate of convergence stated in Proposition 4 is established for the middle interval $[\tau_\ell, \tau_u]$ of $[0, 1]$. However, it becomes significantly more complex for the tail intervals. In this subsection, we show that the rate of convergence for the tails of $\hat{Y}(\tau|\mathbf{x}^*)$ may depend on the nature of the tails, and there is no universal rate of convergence that can cover all cases. To explain this complexity, we consider both the estimation error and the interpolation error at the right endpoint $\tau_{m-1} = 1 - 1/m$ and show how the rates of convergence at this point are affected by the tail characteristics. Please note that the results can also be applied to the left endpoint $\tau_1 = 1/m$ as well.

5.2.1. Estimation Error of $\hat{\beta}_{m-1}$. Notice that, in Section 5.1, the Bahadur representation in Lemma 1 played a critical role in establishing the rate of convergence of $\hat{\beta}_j$ where $\tau_j \in [\tau_\ell, \tau_u]$. However, it only applies to the middle interval. To understand the rate of convergence of $\hat{\beta}_{m-1}$, we need a new Bahadur representation for the extreme quantiles.

The convergence analysis of $\hat{\beta}(\tau)$ as $\tau \rightarrow 0$ or 1 is referred to as extremal quantile regression (Chernozhukov 2005), which employs tools from extreme value theory to study the asymptotic behaviors of the tails in quantile regression. Fortunately, under a certain type of extremal quantile regression called *intermediate order regression quantiles*, i.e., $\tau \rightarrow 1$ and $(1 - \tau)n \rightarrow \infty$ (or $\tau \rightarrow 0$ and $\tau n \rightarrow \infty$ for the left tail), we can still obtain a Bahadur representation, stated in the following lemma. However, due to its reliance on extreme value theory, some preliminaries and technical assumptions are necessary to state this result in a rigorous way, which appears to be a divergence from the main theme of this paper. To enhance the readability, we defer them along with the proof of the lemma to the e-companion. Also, in the lemma, we only state the results on the right tail, while the results on the left tail can be obtained similarly.

LEMMA 5. *Under proper assumptions, if τ satisfies $\tau \rightarrow 1$ and $(1 - \tau)n \rightarrow \infty$ as $n \rightarrow \infty$, we have*

$$\sqrt{\frac{n}{1 - \tau}} f_Y(F_Y^{-1}(\tau|\mathbf{x}^*)|\mathbf{x}^*) \cdot [\hat{\beta}(\tau) - \beta(\tau)] = D_3^{-1} \tilde{W}_n(\tau) + o_{\mathbb{P}}(1),$$

where D_3 is a $p \times p$ matrix and

$$\tilde{W}_n(\tau) = \frac{1}{\sqrt{(1 - \tau)n}} \sum_{i=1}^n \mathbf{x}_i \psi_\tau(y_i - \beta^\top(\tau) \mathbf{x}_i),$$

and $\tilde{W}_n(\tau) \Rightarrow N(0, D_0)$.

Notice that a direct implication of the Bahadur representation of Lemma 5 is that

$$\left\| \hat{\boldsymbol{\beta}}(\tau) - \boldsymbol{\beta}(\tau) \right\| = O_{\mathbb{P}} \left(\frac{\sqrt{1-\tau}}{\sqrt{n} f_Y(F_Y^{-1}(\tau|\mathbf{x}^*)|\mathbf{x}^*)} \right). \quad (11)$$

Compared to Proposition 3, it is clear that the rate of convergence in Equation (11) depends on not only the data size n but also the extremeness of the tail, i.e., $1 - \tau$, and the density at the τ -quantile, i.e., $f_Y(F_Y^{-1}(\tau|\mathbf{x}^*)|\mathbf{x}^*)$.

Now we consider the right endpoint $\tau_{m-1} = 1 - 1/m$ with $1/m \rightarrow 0$ and $n/m \rightarrow \infty$. Then, by Equation (11), it is clear that

$$\left\| \hat{\boldsymbol{\beta}}_{m-1} - \boldsymbol{\beta}(\tau_{m-1}) \right\| = O_{\mathbb{P}} \left(\frac{1}{\sqrt{nm} f_Y(F_Y^{-1}(1-1/m|\mathbf{x}^*)|\mathbf{x}^*)} \right).$$

Therefore, the rate of convergence of $\hat{\boldsymbol{\beta}}_{m-1}$ depends on the tail characteristics of $Y|\mathbf{x}^*$ as well as n and m . To better understand the rate, we consider a simple location shift model,

$$y_i = \boldsymbol{\beta}^T \mathbf{x}_i + \epsilon_i, \quad \epsilon_i \sim_{i.i.d} F_0, \quad (12)$$

and consider three representative distributions of F_0 , i.e., uniform distribution, exponential distribution and Pareto distribution, which correspond to three types of tails in extreme value theory or roughly correspond to distributions with no tail, light tail and heavy tail, respectively (De Haan et al. 2006). In the e-companion we show that all three examples satisfy the assumptions of Lemma 5.

EXAMPLE 1. Suppose that the location shift model (12) and Assumptions 1–3 hold with a compact support \mathcal{X} , $m, n \rightarrow \infty$ and $n/m \rightarrow \infty$.

- Suppose that F_0 follows the uniform distribution on $[0, 1]$. Then,

$$\left\| \hat{\boldsymbol{\beta}}_{m-1} - \boldsymbol{\beta}(\tau_{m-1}) \right\| = O_{\mathbb{P}} \left(\frac{1}{\sqrt{nm}} \right). \quad (13)$$

- Suppose that F_0 follows the exponential distribution with rate $\lambda > 0$. Then,

$$\left\| \hat{\boldsymbol{\beta}}_{m-1} - \boldsymbol{\beta}(\tau_{m-1}) \right\| = O_{\mathbb{P}} \left(\frac{m^{1/2}}{n^{1/2}} \right). \quad (14)$$

- Suppose that F_0 follows the Pareto distribution with tail index $\gamma > 0$, i.e., $F_0(y) = 1 - y^{-\gamma}$ for all $y > 1$. Then,

$$\left\| \hat{\boldsymbol{\beta}}_{m-1} - \boldsymbol{\beta}(\tau_{m-1}) \right\| = O_{\mathbb{P}} \left(\frac{m^{\frac{1}{2} + \frac{1}{\gamma}}}{n^{\frac{1}{2}}} \right). \quad (15)$$

In these three examples, we can clearly see that there is no universal rate of convergence for $\hat{\boldsymbol{\beta}}_{m-1}$ and the rate depends on the tail behaviors. For the uniform distribution, it is faster than that of the middle interval. But for both the exponential distribution and Pareto distribution, it is slower and it depends on the tail index (note that one may view the exponential distribution as a Pareto distribution with $\gamma = \infty$). In general, lighter tail converges faster and heavier tail converges slower. Also, for Pareto distributions, if we set $m = O(\sqrt{n})$, $\hat{\boldsymbol{\beta}}_{m-1}$ may not even converge if $\gamma \leq 2$.

5.2.2. Interpolation Error for $\tau \in (\tau_{m-2}, \tau_{m-1})$. Aside from estimation error, interpolation error is another type of error that the observations generated by QRGMM may have and it also affects the rate of convergence. Similar to the analysis of the estimation error, we only consider the interpolation error near the right endpoint τ_{m-1} . In particular, we analyze the interpolation error for $\tau \in (\tau_{m-2}, \tau_{m-1})$.

Notice that, for $\tau \in (\tau_{m-2}, \tau_{m-1})$, the interpolation error

$$\begin{aligned} & \left| F_Y^{-1}(\tau | \mathbf{x}^*) - \left\{ m(\tau_{m-1} - \tau) F_Y^{-1}(\tau_{m-2} | \mathbf{x}^*) + m(\tau - \tau_{m-2}) F_Y^{-1}(\tau_{m-1} | \mathbf{x}^*) \right\} \right| \\ & \leq \left| F_Y^{-1}(\tau_{m-1} | \mathbf{x}^*) - F_Y^{-1}(\tau_{m-2} | \mathbf{x}^*) \right|, \end{aligned}$$

because $m(\tau_{m-1} - \tau) + m(\tau - \tau_{m-2}) = 1$. Therefore, we may use $\left| F_Y^{-1}(\tau_{m-1} | \mathbf{x}^*) - F_Y^{-1}(\tau_{m-2} | \mathbf{x}^*) \right|$ to understand how the rate of convergence of the interpolation error depends on the tail characteristics. Again we use the same three examples to illustrate this dependence.

EXAMPLE 2. Suppose that the location shift model (12) holds, $m, n \rightarrow \infty$ and $n/m \rightarrow \infty$.

- Suppose that F_0 follows the uniform distribution on $[0, 1]$. Then,

$$\left| F_Y^{-1}(\tau_{m-1} | \mathbf{x}^*) - F_Y^{-1}(\tau_{m-2} | \mathbf{x}^*) \right| = O\left(\frac{1}{m}\right).$$

- Suppose that F_0 follows the exponential distribution with rate $\lambda > 0$. Then,

$$\left| F_Y^{-1}(\tau_{m-1} | \mathbf{x}^*) - F_Y^{-1}(\tau_{m-2} | \mathbf{x}^*) \right| = O(1).$$

- Suppose that F_0 follows the Pareto distribution with tail index $\gamma > 0$. Then,

$$\left| F_Y^{-1}(\tau_{m-1} | \mathbf{x}^*) - F_Y^{-1}(\tau_{m-2} | \mathbf{x}^*) \right| = O(m^{1/\gamma}).$$

In these three examples, we notice some interesting behaviors. First, for the uniform distribution, the interpolation error near the right endpoint has the same rate of convergence as that of the middle interval. Second, for both the exponential distribution and Pareto distribution, the interpolation error does not even converge! This is because the quantile functions of the right tail of both cases explode to infinity very quickly. This further shows that the convergence in distribution that we prove in Section 4 does not imply the sample-path convergence of the generated random variable and the use of the Portmanteau lemma to control the tail probability is critical to the proof (as discussed in Remark 1).

5.3. Uniform Rate of Convergence for the Distribution Function

Section 5.2 shows that there is no universal rate of convergence for the random variable $\hat{Y}(\mathbf{x}^*)$ generated by QRGMM. In this subsection, however, we show that its cumulative distribution function has a uniform rate of convergence, strengthening the uniform convergence result of Corollary 1.

To establish the uniform rate of convergence, we first prove the following lemma. The proof is included in the e-companion, but the critical idea is to notice that $F_{\hat{Y}}(y|\mathbf{x}^*) = 0$ for any $y \in (-\infty, \hat{Y}(\tau_1|\mathbf{x}^*))$, that $F_{\hat{Y}}(y|\mathbf{x}^*) = 1$ for any $y \in (\hat{Y}(\tau_{m-1}|\mathbf{x}^*), +\infty)$, and that $F_{\hat{Y}}(y|\mathbf{x}^*)$ is piece-wise linear for $y \in [\hat{Y}(\tau_1|\mathbf{x}^*), \hat{Y}(\tau_{m-1}|\mathbf{x}^*)]$.

LEMMA 6. *For any given \mathbf{x}^* , and for any given m and n , we have*

$$\sup_{y \in (-\infty, \infty)} |F_{\hat{Y}}(y|\mathbf{x}^*) - F_Y(y|\mathbf{x}^*)| \leq 3 \max_{1 \leq j \leq m-1} \left| F_Y(\hat{Y}(\tau_j|\mathbf{x}^*)|\mathbf{x}^*) - \tau_j \right| + \frac{1}{m}.$$

Lemma 6 shows that, to understand the uniform rate of convergence of the cumulative distribution function of $\hat{Y}(\mathbf{x}^*)$, it is critical to study the uniform rate of convergence of $F_Y(\hat{Y}(\tau_j|\mathbf{x}^*)|\mathbf{x}^*)$ to τ_j for all $j = 1, \dots, m-1$. Notice that, intuitively,

$$\begin{aligned} & \left| F_Y(\hat{Y}(\tau_j|\mathbf{x}^*)|\mathbf{x}^*) - \tau_j \right| \\ &= \left| F_Y(\hat{Y}(\tau_j|\mathbf{x}^*)|\mathbf{x}^*) - F_Y(F_Y^{-1}(\tau_j|\mathbf{x}^*)|\mathbf{x}^*) \right| \approx \left| f_Y(F_Y^{-1}(\tau_j|\mathbf{x}^*)|\mathbf{x}^*) \cdot \left[\hat{Y}(\tau_j|\mathbf{x}^*) - F_Y^{-1}(\tau_j|\mathbf{x}^*) \right] \right| \\ &= \left| f_Y(F_Y^{-1}(\tau_j|\mathbf{x}^*)|\mathbf{x}^*) \cdot \left[\hat{\beta}_j^\top \mathbf{x}^* - \beta(\tau_j)^\top \mathbf{x}^* \right] \right| \leq \left\| f_Y(F_Y^{-1}(\tau_j|\mathbf{x}^*)|\mathbf{x}^*) \cdot \left[\hat{\beta}_j - \beta(\tau_j) \right] \right\| \cdot \|\mathbf{x}^*\|. \end{aligned} \quad (16)$$

Then, by Lemma 5, if $\tau_j \rightarrow 0$ or $\tau_j \rightarrow 1$, $\left| F_Y(\hat{Y}(\tau_j|\mathbf{x}^*)|\mathbf{x}^*) - \tau_j \right| = o_{\mathbb{P}}(1/\sqrt{n})$; while by Lemma 1, if τ_j converges to a value in $(0, 1)$, $\left| F_Y(\hat{Y}(\tau_j|\mathbf{x}^*)|\mathbf{x}^*) - \tau_j \right| = O_{\mathbb{P}}(1/\sqrt{n})$. Therefore, intuitively, the tails are dominated by the middle interval. Then, we have the following theorem, whose more rigorous proof is quite involved and is included in the e-companion.

THEOREM 2. *Suppose that Assumptions 1–3 and the assumptions of Lemma 5 hold. If m satisfies $\frac{1}{m} \rightarrow 0$ and $\frac{n}{m} \rightarrow \infty$ as $n \rightarrow \infty$, then, for any given \mathbf{x}^* , as $m, n \rightarrow \infty$, we have*

$$\sup_{y \in (-\infty, \infty)} |F_{\hat{Y}}(y|\mathbf{x}^*) - F_Y(y|\mathbf{x}^*)| = O_{\mathbb{P}}\left(\frac{1}{\sqrt{n}}\right) + O\left(\frac{1}{m}\right).$$

Theorem 2 shows that even though $\hat{Y}(\mathbf{x})$ does not have a universal rate of convergence, the cumulative distribution function of $\hat{Y}(\mathbf{x})$ does. Moreover, the rate is the same as that of the middle part of $\hat{Y}(\tau|\mathbf{x})$ (Proposition 4). The critical insight lies in Equations (11) and (16). To establish the rate of convergence of the random variable $\hat{Y}(\mathbf{x})$, we need to analyze the rate of convergence of $\left[\hat{\beta}_j - \beta(\tau_j) \right]$ which, by Equation (11), depends on the tail characteristics and may converge slower than the middle interval of the distribution. To establish the uniform rate of convergence of the cumulative distribution function $F_{\hat{Y}}(y|\mathbf{x}^*)$, however, we need the rate of convergence of $f_Y(F_Y^{-1}(\tau_j|\mathbf{x}^*)|\mathbf{x}^*) \cdot \left[\hat{\beta}_j - \beta(\tau_j) \right]$. The existence of the density $f_Y(F_Y^{-1}(\tau_j|\mathbf{x}^*)|\mathbf{x}^*)$ makes the term converges faster than $1/\sqrt{n}$ in the tails, therefore, dominated by the middle interval.

6. Numerical Experiments

In this section, we conduct a series of numerical experiments to evaluate the performance of QRGMM, validate its asymptotic properties, and demonstrate its practical utility. We also compare it with the state-of-the-art CWGAN with gradient penalty (CWGAN-GP) (Athey et al. 2021), which is a variant of GAN that aims to learn the conditional distribution using the Wasserstein loss function and gradient penalty. Previous research (Gulrajani et al. 2017, Zheng et al. 2020) has indicated that CWGAN-GP can significantly improve the performances of GAN and CGAN. However, our numerical results suggest that QRGMM not only surpasses CWGAN-GP in performance but also exhibits superior robustness for simulation generative metamodeling problems. For convenience, we refer to the latter algorithm simply as CWGAN in the rest of this paper.

This section is structured as follows. Firstly, we utilize synthetic datasets to compare the performance of QRGMM and CWGAN, under the conditions where Assumption 1 is either satisfied or violated. We also validate the convergence and rate of convergence of QRGMM. Subsequently, we assess the practical effectiveness of QRGMM and CWGAN using a realistic simulator. We demonstrate how QRGMM can expedite the simulation process and facilitate real-time decision-making. The experiments are conducted on a computer with two Intel Xeon Gold 6248R CPUs (each with 24 cores), 256GB RAM, and two NVIDIA GeForce RTX 3090 GPUs.

Recall that the goal of generative metamodeling is to build a “fast simulator of the simulator” capable of generating a large number of observations almost instantaneously to support real-time decision-making. Our numerical study consistently demonstrates that both QRGMM and CWGAN achieve this objective impressively. For all the experiments reported in Sections 6.1 and 6.2, generating 10^5 observations from the generative models require *less than 0.2 seconds* of computational time for CWGAN and *less than 0.05 seconds* for QRGMM. Therefore, for all experiments, we set $K = 10^5$ to estimate any summary statistics, where K is the number of observations generated by the generative model. This specification virtually eliminates all estimation errors once the generative models are established.

6.1. Experiments on Synthetic Data

In this subsection, we assume that we know the true distribution of $Y(\mathbf{x})$. Hence, we can test the performance of QRGMM and validate its asymptotic properties conveniently, using the data generated from the true distributions (called synthetic data).

6.1.1. Performance Comparisons. To compare the performance of QRGMM and CWGAN, We consider the following two scenarios:

Scenario 1: Let $\mathbf{x} = (1, x_1, x_2, x_3)^\top$. We assume that $Y|\mathbf{x}$ follows a normal distribution with mean $\mu(\mathbf{x})$ and standard deviation $\sigma(\mathbf{x})$ where $\mu(\mathbf{x}) = 5 + x_1 + 2x_2 + 0.5x_3$ and $\sigma(\mathbf{x}) = 1 + 0.1x_1 + 0.2x_2 + 0.05x_3$. Then, the conditional quantile $F_Y^{-1}(\tau|\mathbf{x})$ with $\tau \in (0, 1)$ satisfies

$$F_Y^{-1}(\tau|\mathbf{x}) = \mu(\mathbf{x}) + \sigma(\mathbf{x})z_\tau = 5 + z_\tau + (1 + 0.1z_\tau)x_1 + (2 + 0.2z_\tau)x_2 + (0.5 + 0.05z_\tau)x_3,$$

where z_τ is the τ -quantile of the standard normal distribution. Therefore, it satisfies Assumption 1.

Scenario 2: Let $\mathbf{x} = (1, x_1, x_2)^\top$. We assume that $Y|\mathbf{x}$ follows a Laplace distribution (also known as a double exponential distribution) with the location parameter $\mu(\mathbf{x})$ and scale parameter $b(\mathbf{x})$ where $\mu(\mathbf{x}) = 0.05x_1x_2$ and $b(\mathbf{x}) = 5 \sin^2(x_1 + x_2) + 5$. Then, the conditional quantile $F_Y^{-1}(\tau|\mathbf{x})$ with $\tau \in (0, 1)$ satisfies

$$F_Y^{-1}(\tau|\mathbf{x}) = \mu(\mathbf{x}) + b(\mathbf{x})\zeta_\tau = 0.05x_1x_2 + [5 \sin^2(x_1 + x_2) + 5] \zeta_\tau,$$

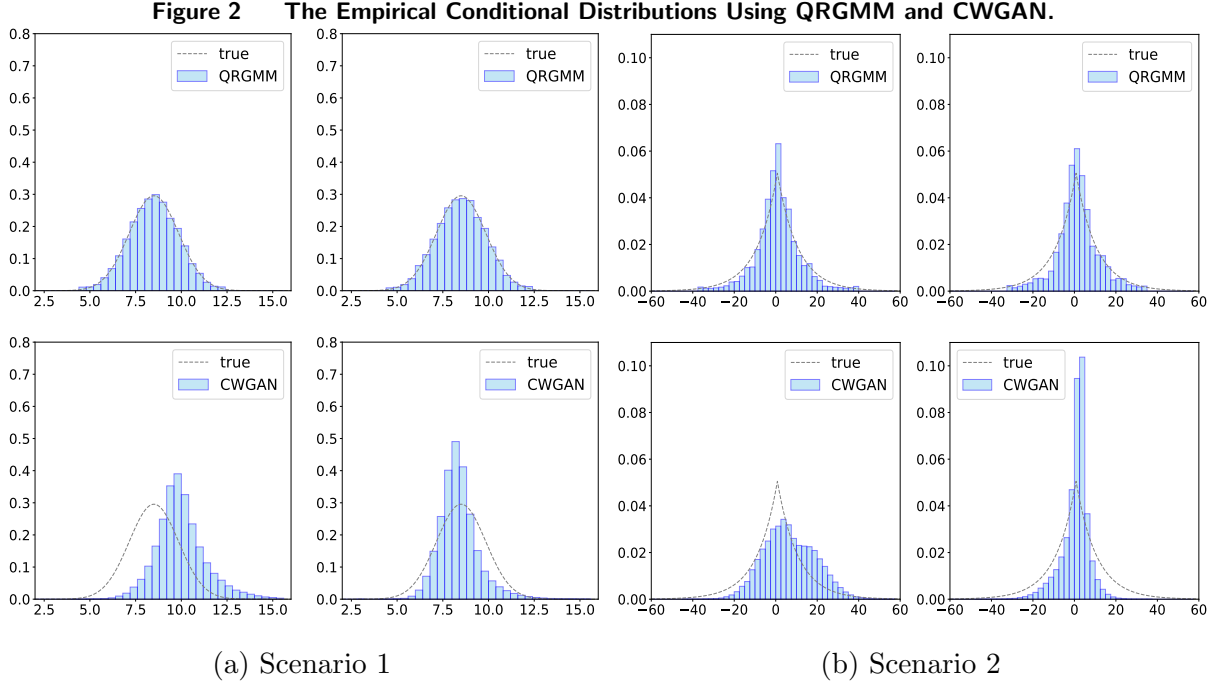
where ζ_τ is the τ -quantile of the Laplace(0, 1) distribution. Therefore, it violates Assumption 1.

To generate data from the above two scenarios, we let \mathbf{x} follow Unif($1 \times [0, 10] \times [-5, 5] \times [0, 5]$) distribution in Scenario 1 and \mathbf{x} follow Unif($1 \times [0, 10] \times [-5, 5]$) distribution in Scenario 2. For QRGMM, we fit the linear quantile regression models $F_Y^{-1}(\tau|\mathbf{x}) = \boldsymbol{\beta}(\tau)^\top \mathbf{x}$ in Scenario 1, and fit the approximate linear quantile regression models $F_Y^{-1}(\tau|\mathbf{x}) = \boldsymbol{\beta}(\tau)^\top \mathbf{b}(\mathbf{x})$ in Scenario 2, where $\mathbf{b}(\mathbf{x})$ is the third-order polynomial basis functions, i.e., $\mathbf{b}(\mathbf{x}) = [1, x_1, x_2, x_1^2, x_1x_2, x_2^2, x_1^3, x_1^2x_2, x_1x_2^2, x_2^3]$.

To test the performance of QRGMM and CWGAN, we generate $\{(\mathbf{x}_i, y_i)\}_{i=1}^n$ from the above two scenarios to train the respective generative metamodells. Then, given a new input \mathbf{x}^* , we generate K observations of $\hat{y}(\mathbf{x}^*)$ using the generative metamodells and compare their empirical conditional distributions with the true distributions. In particular, in the experiments, we set $n = 10^4$ and $K = 10^5$. For QRGMM, we set $m = 300$; for CWGAN, we set `batch_size` = 4096, suggested by Athey et al. (2021), and `max_epochs` = 500 after tuning.

We present the results of two replications in Figure 2. From these results, it is clear that the observations generated by QRGMM exhibit a closer resemblance to the true distributions in both scenarios, while the ones generated by CWGAN deviate significantly from the true distributions. Furthermore, there are notable discrepancies between the two replications of CWGAN, whereas QRGMM shows much smaller discrepancies, suggesting that QRGMM is a more robust generative metamodel. Finally, the observations generated by CWGAN show a mode collapse phenomenon, i.e., the observations are more likely to be concentrated in a limited subset of the distribution, which is well known in the GAN literature (Saxena and Cao 2021).

However, the results reported in Figure 2 may depend on the new input vector \mathbf{x}^* and on the replications. To provide a more holistic comparison of the two generative metamodells, we take



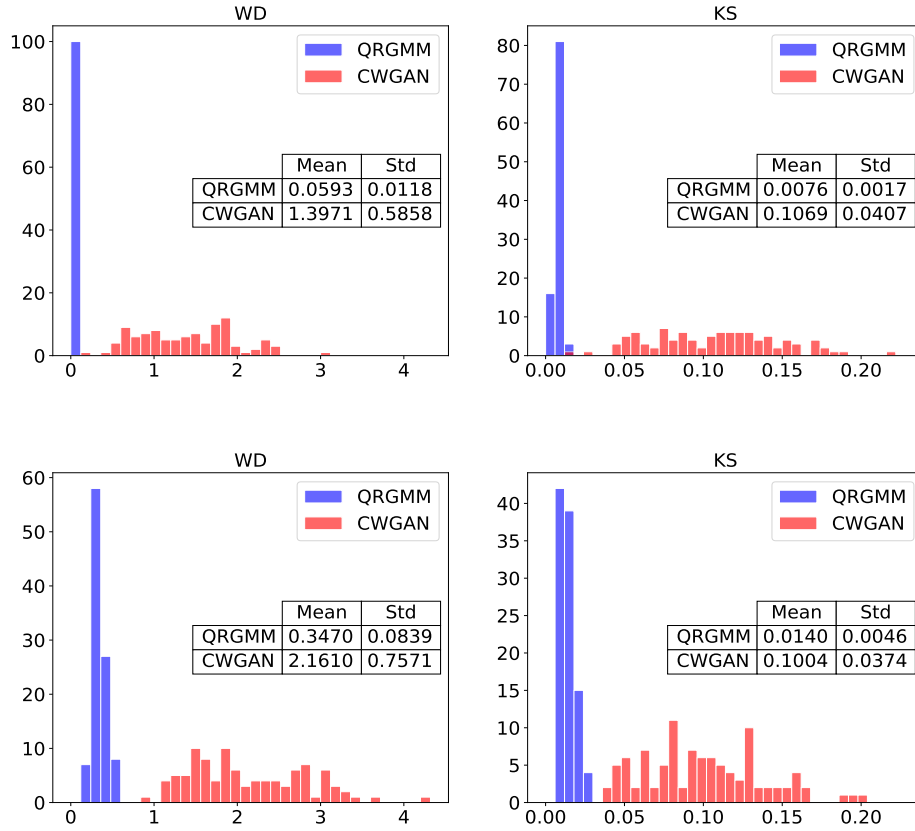
Note. In scenario 1, $\mathbf{x}^* = (1, 4, -1, 3)$, and in scenario 2, $\mathbf{x}^* = (1, 4, 4)$. For each scenario, we show two replications.

an “unconditional” perspective. Specifically, we generate a set of data $\{(\mathbf{x}'_i, y'_i)\}_{i=1}^n$ from the true distribution, and use the trained generative metamodel to simulate a set of data with the same data size and the same \mathbf{x} values, i.e., $\{(\mathbf{x}'_i, \hat{y}'_i)\}_{i=1}^n$. Then, we can compare the statistical properties of the two datasets, one from the true distribution and the other from the generative models. We may replicate this experiment multiple times and calculate certain summary statistics. Here we use the means and standard deviations of the sample means of $\{y'_i\}_{i=1}^n$ and $\{\hat{y}'_i\}_{i=1}^n$ by QRGMM and CWGAN, calculated over 100 replications, and report them in Table 1. We also consider the *Wasserstein distance* (WD, see Arjovsky et al. (2017)) and *K-S statistic* (KS, see Massey Jr (1951)), both of which are important measures that quantify the distance between two probability distributions. We calculate them for each replication and report the histograms and summary statistics over 100 replications in Figure 3.

From Table 1, we see that the summary statistics of the QRGMM-generated data are significantly closer to the statistics of the real data than those of the CWGAN-generated data. In particular, we see that the data generated by CWGAN show significantly more variations across replications in both scenarios, as depicted by the standard deviations of the sample means, showing that the data generated by CWGAN are not robust. The same conclusions can also be drawn from Figure 3, where we see that not only the data generated by QRGMM have smaller WD and KS values, but they also have much smaller variations.

Table 1 Means and Standard Deviations of 100 Sample Means.

	Scenario 1		Scenario 2	
	Mean	Std	Mean	Std
Truth	11.2469	0.0633	-0.0009	0.1056
QRGMM	11.2518	0.0667	-0.0122	0.1341
CWGAN	11.3654	1.2863	0.2044	1.8438

Figure 3 Histograms, Means and Standard Deviations of WD and KS.

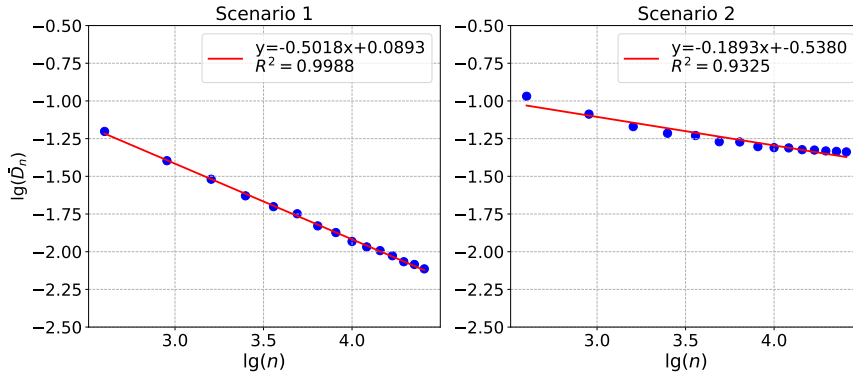
Note. WD and KS are calculated between the empirical distributions of $\{y'_i\}_{i=1}^n$ and $\{\hat{y}'_i\}_{i=1}^n$ by QRGMM and CWGAN over 100 replications for Scenario 1 (top row) and Scenario 2 (bottom row).

6.1.2. Convergence in Distribution. In this part, we validate the convergence of QRGMM in distribution established in Section 4. We use the former Scenarios 1 and 2 to test the convergence in distribution. By Corollary 1, we know that the convergence in distribution implies the uniform convergence of cumulative distribution functions. Therefore, we use the K-S statistic to test the uniform convergence of the cumulative distribution functions. Compared with the Wasserstein distance, the K-S statistic can measure not only the distance between two empirical distributions (two-sample test) but also the distance between an empirical distribution and a known distribution

(one-sample test) directly. After training the generative metamodel, we can generate many random observations $\hat{y}(\mathbf{x}^*)$ given a fixed input \mathbf{x}^* and calculate the K-S statistic between the empirical distribution $\tilde{F}_Y(\cdot|\mathbf{x}^*)$ of these random observations and the true distribution $F_Y(\cdot|\mathbf{x}^*)$. Specifically, we use the known distribution to generate a sequence of datasets whose data size $n = 20^2, 30^2, \dots, 160^2$, and then we use these data to train QRGMM where we set $m = \sqrt{n}$. Next, given a new \mathbf{x}^* , we use the trained QRGMM to generate $K = 10^5$ random observations. Finally, we calculate the K-S statistic between the generated observations and the true conditional distribution $F_Y(\cdot|\mathbf{x}^*)$, denoted as D_n . We replicate the experiment 100 times, calculate the average \bar{D}_n , and plot $\log \bar{D}_n$ with respect to $\log n$. Notice that the slope of the log-log curve represents the rate of convergence.

For Scenario 1, we set $\mathbf{x}^* = (1, 6, 1, 2)$. Figure 4 shows that the distributions of the QRGMM-generated data indeed converge and its rate of convergence is close to the theoretical value of $-\frac{1}{2}$ with R^2 approximating 1. For Scenario 2, we set $\mathbf{x}^* = (1, 7, 2)$. Figure 4 shows that \bar{D}_n stops decreasing when n is large enough. It makes sense because Assumption 1 does not hold and there is a model error caused by the polynomial approximation. We also repeat the convergence tests using the CWGAN-generated data for both Scenarios 1 and 2 and include the results in the e-companion. There is no sign of convergence for the CWGAN-generated data.

Figure 4 $\log \bar{D}_n$ v.s. $\log n$ for Scenarios 1 and 2.



6.1.3. Rate of Convergence. Next, we validate the rate-of-convergence results of QRGMM established in Section 5. In particular, we analyze the rates of convergence for the middle interval, the tail endpoint and the distribution function. We assume the true model is a simple location shift model $Y = 1 + 0.5\mathbf{x} + \varepsilon$ and ε may take three distributions, the uniform distribution on $[0, 1]$, the exponential distribution with $\lambda = 1$, and the Pareto distribution with $\gamma = 1$. When generating the true data, we assume \mathbf{x} follows the uniform distribution on $[-2, 2]$. Throughout the experiments reported in this part, we train QRGMM using $n = 20^2, 30^2, \dots, 160^2$ true data points with $m = \sqrt{n}$,

generate $K = 10^5$ observations from the trained QRGMM at $\mathbf{x}^* = 1$ to study distribution behaviors of the generated data, and repeat this process for 100 replications to compute the summary statistics.

First, we validate the rate of convergence for the middle interval established by Proposition 4. This proposition asserts that, for any given \mathbf{x}^* , as $n, m \rightarrow \infty$,

$$\sup_{\tau \in [\tau_\ell + \frac{1}{m}, \tau_u - \frac{1}{m}]} |\hat{Y}(\tau|\mathbf{x}^*) - F_Y^{-1}(\tau|\mathbf{x}^*)| = O_{\mathbb{P}}\left(\frac{1}{\sqrt{n}}\right) + O\left(\frac{1}{m}\right).$$

We set $\tau_\ell = 0.25$ and $\tau_u = 0.75$, estimate $\sup_{\tau \in [\tau_\ell + \frac{1}{m}, \tau_u - \frac{1}{m}]} |\hat{Y}(\tau|\mathbf{x}^*) - F_Y^{-1}(\tau|\mathbf{x}^*)|$ using the observations generated by QRGMM for each replication, and denote their average over 100 replications by \bar{E}_n . Then, we plot $\log \bar{E}_n$ with respect to $\log n$ for three distributions of ε in the top row of Figure 5. It is clear that, for all three distributions, the empirical rates of convergence are close to the theoretical rate of $1/\sqrt{n}$.

Second, we validate the rate of convergence for the tail endpoint established by Lemma 5. Here, we estimate $|\hat{Y}(\tau_{m-1}|\mathbf{x}^*) - F_Y^{-1}(\tau_{m-1}|\mathbf{x}^*)|$ using the observations generated by QRGMM, denote the average over 100 replications by \bar{E}'_n , and plot $\log \bar{E}'_n$ with respect to $\log n$ for three distributions of ε in the middle row of Figure 5. It is clear that, for all three distributions, the empirical rates of convergence match their theoretical rates of $n^{-3/4}$, $n^{-1/4}$ and $n^{1/4}$, derived in Section 5.2.

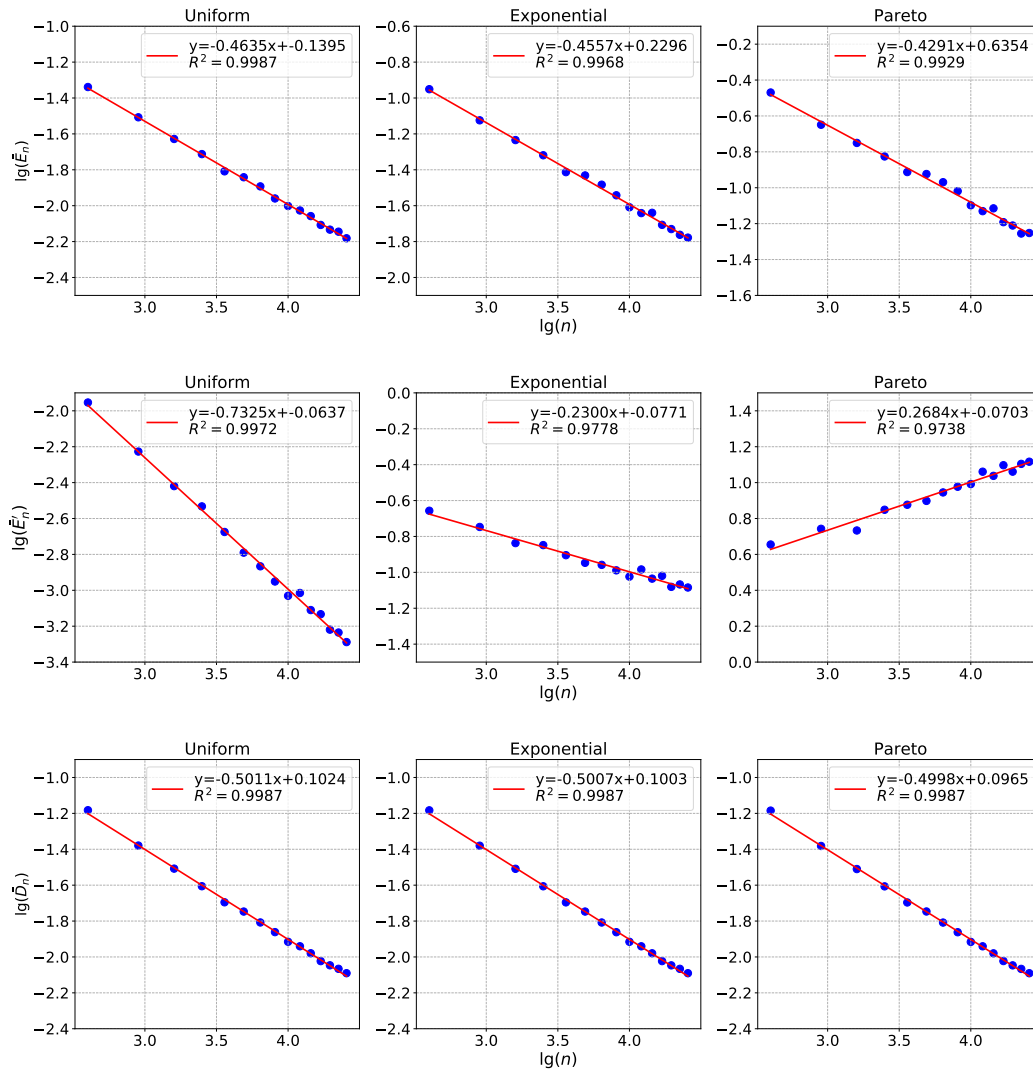
Third, we validate the uniform rate of convergence of the distribution established by Theorem 2. Here, we use the average K-S statistic \bar{D}_n , which is also used in Section 6.1.2. we plot $\log \bar{D}_n$ with respect to $\log n$ for three distributions of ε in the bottom row of Figure 5. It is clear that, for all three distributions, the empirical rates of convergence match the theoretical rate of $n^{-1/2}$ very well.

Finally, we analyze the effect of m and show why $m = O(\sqrt{n})$ is advisable. We use Scenario 1 of Section 6.1.1, set $n = 10^4$ and $m = 10^1, 10^{1.25}, \dots, 10^{3.75}, 10^4$. After training QRGMM, given $\mathbf{x}^* = (1, 6, 1, 2)$, we generate $K = 10^5$ random observations and calculate the average K-S statistic \bar{D}_m over 100 replications. Figure 6 shows that the \bar{D}_m changes relatively little after m increases to $\sqrt{n} = 100$. The experimental and theoretical results both tell us that $m = O(\sqrt{n})$ is a good choice, taking into account the factors of computation cost and computation time.

6.2. Experiments on a Practical Simulator

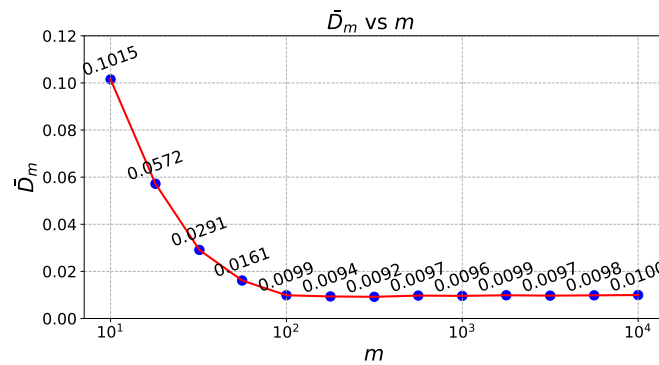
In this subsection, we apply the proposed generative metamodelling to an *esophageal cancer Markov chain simulation model*, developed and calibrated by domain experts in cancer research. The simulation model was introduced by Hur et al. (2004) and Choi et al. (2014), in which the model is developed and studied for the effectiveness of aspirin and statin chemopreventions against *esophageal adenocarcinoma* (EAC), as well as for some strategies of *Barrett's esophagus* (BE) management. The incidence of EAC, a predominant subtype of esophageal cancer, has increased by 500% in the past 40 years (Choi et al. 2014). It is widely acknowledged that aspirin and statin are efficacious

Figure 5 The Rates of Convergence.



Note. We show the rates of convergence for the middle intervals (top row), the tail endpoint (middle row) and the distribution (bottom row).

Figure 6 Effect of m on the Error.



in reducing the progression from BE to EAC, given that BE serves as a precursor lesion to EAC (Kastelein et al. 2011). Various factors, such as age, weight, and lifestyle habits, influence the cancer progression rate in BE patients. Besides, patients’ responses to drugs may vary based on their drug resistance and tolerance. This model allows for the simulation of quality-adjusted life years (QALYs) in BE patients undergoing different treatment regimens by modeling transitions among various health states until death. This model has been used as a standard test problem for ranking and selection with covariates (R&S-C, Shen et al. (2021) and Li et al. (2022)) and its details may be found at the simulation optimization repository on github (<https://simopt.github.io/ECSim>). But it is also important to note that the run time of this model is also very short, compared to simulation models used in practice. It is used only to evaluate learning-based algorithms, such as the R&S-C algorithms or our algorithms.

The model has four inputs: x_1 is the starting age of a treatment regimen, $x_1 \in [55, 80]$ as documented by Naef and Savary (1972), there is a peak incidence of BE in individuals within this age range; x_2 is the risk factor that denotes the annual progression rate of BE to EAC, $x_2 \in [0, 0.1]$ following the specification in Hur et al. (2004); x_3 and x_4 are the progression reduction effects of aspirin and statin, X_3 and $X_4 \in [0, 1]$ by definition. We use $\mathbf{x} = (x_1, x_2, x_3, x_4)^\top$ to denote the input vector. The model has two alternative outputs $Y_1(\mathbf{x})$ and $Y_2(\mathbf{x})$, which are the QALY of the BE patient when aspirin and statin are used, respectively.

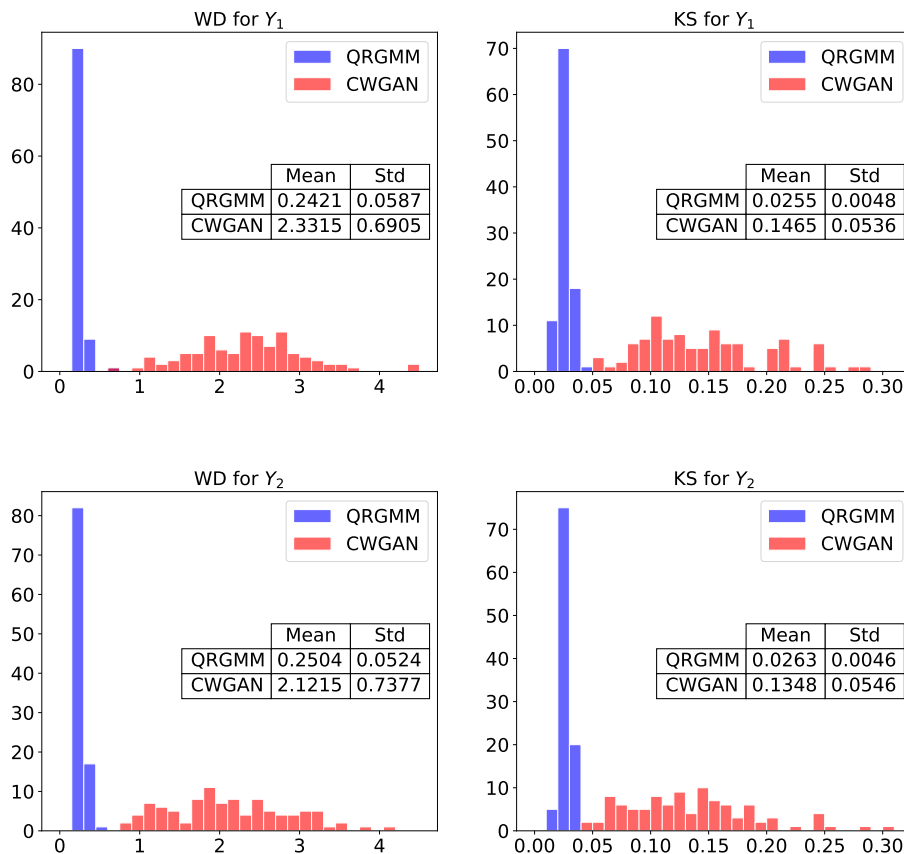
In this subsection, we apply both QRGMM and CWGAN to build generative metamodellers for both $Y_1(\mathbf{x})$ and $Y_2(\mathbf{x})$. We study the performance of these metamodellers and demonstrate their utility in selecting the better personalized treatment between aspirin and statin chemopreventions. The dataset $\{(\mathbf{x}_i, y_{1i}), (\mathbf{x}_i, y_{2i})\}_{i=1}^n$ with $n = 10^4$ are constructed through independent simulated copies of the random vector $(\mathbf{x}, Y_1(\mathbf{x}))$ and $(\mathbf{x}, Y_2(\mathbf{x}))$, where \mathbf{x} is uniformly distributed on its feature space. For QRGMM, we use the following general linear quantile regression model $F_Y^{-1}(\tau|\mathbf{x}) = \boldsymbol{\beta}(\tau)^\top \mathbf{b}(\mathbf{x})$, with the basis $\mathbf{b}(\mathbf{x}) = (1, x_1, x_2, x_3, x_4, x_1^2, x_2^2, x_3^2, x_4^2, x_1x_2, x_1x_3, x_1x_4, x_2x_3, x_2x_4, x_3x_4)^\top$, which admits the interaction effects between different inputs in the model, and we set $m = 300$. For CWGAN, we set `max_epochs` = 4500 and 4000 for $Y_1(\mathbf{x})$ and $Y_2(\mathbf{x})$ respectively after tuning and keep the other hyperparameters consistent with those in Section 6.1.1.

Similar to Section 6.1.1, we replicate the experiments of the generative metamodellers 100 times and summarize the same unconditional performance measures for Y_1 and Y_2 in Table 2 and Figure 7. These results again show that QRGMM is more effective and more robust than CWGAN.

6.2.1. Estimating and Ordering Mean Treatment Effects. With the trained generative metamodellers, once the covariates are observed, one can use them to generate observations quickly and use the observations to calculate summary statistics and to make decisions. First, we consider

Table 2 Means and Standard Deviations of Sample Means.

	Y_1		Y_2	
	Mean	Std	Mean	Std
Truth	15.6124	0.0987	15.6163	0.1060
QRGMM	15.6545	0.1070	15.6868	0.1028
CWGAN	15.5920	1.9483	15.4783	1.8889

Figure 7 Histograms, Means and Standard Deviations of WD and KS.

Note. WD and KS are calculated between the empirical distributions of $\{y'_{1i}\}_{i=1}^n$ and $\{\hat{y}'_{1i}\}_{i=1}^n$ by QRGMM and CWGAN for Y_1 , and $\{y'_{2i}\}_{i=1}^n$ and $\{\hat{y}'_{2i}\}_{i=1}^n$ by QRGMM and CWGAN for Y_2 over 100 replications.

the estimation of the mean treatment effects and their ordering. Suppose that a patient comes and we observe his covariates $\mathbf{x}^* = (1, 70, 0.05, 0.2, 0.8)$. Based on the generative metamodels, we can quickly generate $K = 10^5$ observations for $Y_1(\mathbf{x}^*)$ and $Y_2(\mathbf{x}^*)$ and compute their sample means $\bar{Y}_1(\mathbf{x}^*)$ and $\bar{Y}_2(\mathbf{x}^*)$ and order them. We repeat the experiments 100 times, and calculate the means and standard deviations of 100 sample means for two different treatment regimens and estimate the number of correct ordering¹, and report them in Table 3. For comparison purpose, we also

¹ In this example, based on a very large number of observations generated at \mathbf{x}^* by the true simulator, we know that treatment 2 is better than treatment 1.

conduct the same experiments using the true data (of size $n = 10,000$) generated by the simulator at \mathbf{x}^* , which takes significantly more time. Additionally, we compare our results with those obtained from a traditional metamodeling method that utilizes a linear regression model to learn the mean surface (denoted as LR). To ensure fairness in our comparison, we employ same polynomial basis functions for LR and QRGMM. The corresponding findings are also presented in Table 3. From these results, it is clear that the data generated by QRGMM may be used to estimate and compare the means of $Y_1(\mathbf{x}^*)$ and $Y_2(\mathbf{x}^*)$, producing similar results compared to the real data and traditional metamodeling method. Furthermore, it has significantly better performance than CWGAN.

Table 3 Means and Standard Deviations of $\bar{Y}_1(\mathbf{x}^*)$ and $\bar{Y}_2(\mathbf{x}^*)$ and the Number of Correct Ordering.

	$\mathbb{E}[\bar{Y}_1(\mathbf{x}^*)]$	$\mathbb{E}[\bar{Y}_2(\mathbf{x}^*)]$	Std $[\bar{Y}_1(\mathbf{x}^*)]$	Std $[\bar{Y}_2(\mathbf{x}^*)]$	# correct ordering
Simulator	13.45	14.01	0.08	0.07	100
QRGMM	13.47	14.04	0.20	0.18	100
LR	13.47	14.04	0.20	0.19	98
CWGAN	13.30	14.12	1.44	1.64	67

The number of correct ordering is the number of $\bar{Y}_1(\mathbf{x}^*) < \bar{Y}_2(\mathbf{x}^*)$ among 100 replications.

In addition, we record the computational times of generating 10^5 observations by QRGMM and CWGAN in Table 4. We notice that both of them are very fast, with QRGMM faster than CWGAN. From a practical viewpoint, the generation times of both algorithms are negligible, so that they may be used in practice to make real-time decisions.

Table 4 Average Total Sampling Time over 100 Replications.

	Total time for $Y_1(\mathbf{x}^*)$	Total time for $Y_2(\mathbf{x}^*)$
QRGMM	0.0357s	0.0351s
CWGAN	0.1734s	0.1744s

For $K = 10^5$ observations of $Y_1(\mathbf{x}^*)$ and $Y_2(\mathbf{x}^*)$.

6.2.2. Ranking and Selection with Covariates. Second, we consider the problem of selecting the best treatment for individual patients. The problem is typically formulated as a R&S-C problem, in which a policy is learned based on offline simulation experiments and is subsequently utilized to make online selection decisions. This is because, more often than not, there is insufficient time to conduct simulation experiments after the covariates have been identified (Shen et al. 2021). However, when generative metamodels are available, generating observations from the metamodels is extremely fast. Consequently, we can generate a large number of observations from every alternative treatment and compare their sample means, *after the covariates have been identified*.

We use QRGMM and CWGAN to generate $K = 10^5$ observations for each alternative and compare their means to solve the R&S-C problem, and compare them to the TS^+ procedure, a R&S-C procedure proposed by Shen et al. (2021). For comparison purpose, we also apply the KN procedure of Kim and Nelson (2001) using the observations from the true simulator after the covariates are identified.² We use the average probability of correct selection (PCS_E) of Shen et al. (2021) to compare different algorithms. The PCS_E may be estimated by

$$\widehat{\text{PCS}}_E = \frac{1}{R} \sum_{r=1}^R \frac{1}{T} \sum_{t=1}^T \mathbb{I} \left\{ \mu_{i^*(\mathbf{x}_t)}(\mathbf{x}_t) - \mu_{\hat{i}_r^*(\mathbf{x}_t)}(\mathbf{x}_t) < \delta \right\},$$

where in our experiments, the replication number $R = 100$, the covariates number $T = 100$, the indifference-zone parameter $\delta = 1/6$ (2 months), the optimal choice $i^*(\mathbf{x}_t)$ and its mean $\mu_{i^*(\mathbf{x}_t)}(\mathbf{x}_t)$ for covariates \mathbf{x}_t are obtained through a brute-force simulation, the selected choice $\hat{i}_r^*(\mathbf{x}_t)$ is obtained through the above four procedures, and the covariates \mathbf{x}_t are sampled uniformly in its feature space. In the experiments, the target PCS_E is set to 95% for the TS^+ procedure, the number of observations used for training generative metamodels is $n = 10^5$ (which is comparable to the number of observations used by the TS^+ procedure), and the number of alternatives is 2. We set $m=300$ for QRGMM, and `max_epochs` = 500 for CWGAN.

The results are reported in Table 5. From the results, we observe that the performance of QRGMM is comparable to those of the TS^+ procedure and the KN procedure, all of which are above the target level of 95%. This demonstrates the capability of QRGMM in facilitating real-time decision-making. In contrast, the performance of CWGAN is not satisfactory, showing that the distributions it learns are not accurate enough to facilitate real-time decision-making in typical simulation studies.

	TS^+	KN+Simulator	QRGMM	CWGAN
$\widehat{\text{PCS}}_E$	0.9946	0.9952	0.9858	0.7454

It is important to point out that R&S-C procedures need to know what summary statistics are used at the offline stage. For instance, the TS^+ procedure only selects the best mean performance. In practice, however, decision makers may only know the summary statistic after identifying the covariates. For instance, in the esophageal simulation example, a patient may choose to use summary statistics other than the means to decide what treatment to use. In this scenario, R&S-C procedures may not be used, but generative metamodels can always be used no matter what summary statistic or even multiple summary statistics are used for comparisons.

² Notice that this approach typically takes a lot of time and it is not practical for online decision-making.

7. Conclusions and Future Research

In this paper, we introduce a new concept known as generative metamodeling, which exploits offline simulation to construct a “faster simulator of the simulator” for real-time decision-making. To put this concept into practice, we develop the QRGMM algorithm, establish its convergence in distribution, and analyze its rate of convergence. Through a series of carefully designed numerical experiments, we assess its empirical performance and compare it with the state-of-the-art conditional generative algorithm, CWGAN-GP. Our findings indicate that the data generated by QRGMM effectively capture the true distributions and significantly outperform data generated by CWGAN-GP. Moreover, the negligible data generation time of QRGMM makes it a practical tool for real-time decision-making.

This paper is the first to investigate the significant role generative metamodeling could play in stochastic simulation. There are numerous potential directions for future research. First, many simulation models produce a vector of output variables. Hence, extending QRGMM to handle multi-dimensional simulation output and capture their dependence structure is an important research question. Second, the quantile regression model used in this paper assumes a (linear) parametric structure, which may introduce modeling errors that are not easy to remove. Therefore, exploring nonparametric quantile regression models, such as stochastic kriging or neural networks, in generative metamodels to mitigate these modeling errors is another interesting research question. Last but not least, identifying practical applications where generative metamodeling techniques can be particularly beneficial is also crucial.

References

- Arjovsky M, Chintala S, Bottou L (2017) Wasserstein generative adversarial networks. *Proceedings of the 34th International Conference on Machine Learning*, 214–223.
- Athey S, Imbens GW, Metzger J, Munro E (2021) Using wasserstein generative adversarial networks for the design of monte carlo simulations. *Journal of Econometrics* .
- Bahadur RR (1966) A note on quantiles in large samples. *Annals of Mathematical Statistics* 37(3):577–580.
- Banks J, Carson JS, Nelson BL, Nicol DM (2009) *Discrete-Event System Simulation* (Pearson), 5th edition.
- Barton RR (2020) Tutorial: Metamodeling for simulation. *Proceedings of the 2020 Winter Simulation Conference*, 1102–1116.
- Ben Taieb S (2022) Learning quantile functions for temporal point processes with recurrent neural splines. *Proceedings of the 25th International Conference on Artificial Intelligence and Statistics*, 3219–3241.
- Bengio Y, Ducharme R, Vincent P, Jauvin C (2003) A neural probabilistic language model. *Journal of Machine Learning Research* 3(Feb):1137–1155.

- Chen X, Kim KK (2016) Efficient VaR and CVaR measurement via stochastic kriging. *INFORMS Journal on Computing* 28(4):629–644.
- Chernozhukov V (2005) Extremal quantile regression. *Annals of Statistics* 33(2):806–839.
- Choi SE, Perzan KE, Tramontano AC, Kong CY, Hur C (2014) Statins and aspirin for chemoprevention in Barrett’s esophagus: Results of a cost-effectiveness analysis. *Cancer Prevention Research* 7(3):341–350.
- Chu F, Nakayama MK (2012) Confidence intervals for quantiles when applying variance-reduction techniques. *ACM Transactions on Modeling and Computer Simulation* 22(2):1–25.
- Dabney W, Ostrovski G, Silver D, Munos R (2018a) Implicit quantile networks for distributional reinforcement learning. *Proceedings of the 35th International Conference on Machine Learning*, 1096–1105.
- Dabney W, Rowland M, Bellemare M, Munos R (2018b) Distributional reinforcement learning with quantile regression. *Proceedings of the 32nd AAAI Conference on Artificial Intelligence*, 2892–2901.
- De Haan L, Ferreira A, Ferreira A (2006) *Extreme Value Theory: An Introduction* (Springer).
- Goodfellow I, Pouget-Abadie J, Mirza M, Xu B, Warde-Farley D, Ozair S, Courville A, Bengio Y (2014) Generative adversarial nets. *Advances in Neural Information Processing Systems 27*, 2672–2680.
- Gouttes A, Rasul K, Koren M, Stephan J, Naghibi T (2021) Probabilistic time series forecasting with implicit quantile networks. *arXiv preprint arXiv:2107.03743* .
- Gulrajani I, Ahmed F, Arjovsky M, Dumoulin V, Courville AC (2017) Improved training of Wasserstein GANs. *Advances in Neural Information Processing Systems 30*, 5769–5779.
- Hannah LA, Powell WB, Blei DM (2010) Nonparametric density estimation for stochastic optimization with an observable state variable. *Advances in Neural Information Processing Systems 23*, 820–828.
- Ho J, Jain A, Abbeel P (2020) Denoising diffusion probabilistic models. *Advances in Neural Information Processing Systems 33*, 6840–6851.
- Hong LJ, Jiang G (2019) Offline simulation online application: A new framework of simulation-based decision making. *Asia-Pacific Journal of Operational Research* 36(6):1940015.
- Hur C, Nishioka NS, Gazelle GS (2004) Cost-effectiveness of aspirin chemoprevention for Barrett’s esophagus. *Journal of the National Cancer Institute* 96(4):316–325.
- Jiang G, Hong LJ, Nelson BL (2020) Online risk monitoring using offline simulation. *INFORMS Journal on Computing* 32(2):356–375.
- Kastelein F, Spaander MC, Biermann K, Steyerberg EW, Kuipers EJ, Bruno MJ, study Group P, et al. (2011) Nonsteroidal anti-inflammatory drugs and statins have chemopreventative effects in patients with barrett’s esophagus. *Gastroenterology* 141(6):2000–2008.
- Kim SH, Nelson BL (2001) A fully sequential procedure for indifference-zone selection in simulation. *ACM Transactions on Modeling and Computer Simulation* 11(3):251–273.

-
- Kingma DP, Welling M (2013) Auto-encoding variational bayes. *arXiv preprint arXiv:1312.6114* .
- Koenker R (2005) *Quantile Regression* (Cambridge University Press).
- Koenker R (2017) Computational methods for quantile regression. Koenker R, Chernozhukov V, He X, Peng L, eds., *Handbook of Quantile Regression*, 55–67 (Chapman and Hall/CRC).
- Li H, Lam H, Peng Y (2022) Efficient learning for clustering and optimizing context-dependent designs. *Operations Research*, forthcoming.
- Massey Jr FJ (1951) The Kolmogorov-Smirnov test for goodness of fit. *Journal of the American statistical Association* 46(253):68–78.
- Mirza M, Osindero S (2014) Conditional generative adversarial nets. *arXiv preprint arXiv:1411.1784* .
- Mnih V, Kavukcuoglu K, Silver D, Rusu AA, Veness J, Bellemare MG, Graves A, Riedmiller M, Fidjeland AK, Ostrovski G, et al. (2015) Human-level control through deep reinforcement learning. *Nature* 518(7540):529–533.
- Naef A, Savary M (1972) Conservative operations for peptic esophagitis with stenosis in columnar-lined lower esophagus. *Annals of Thoracic Surgery* 13(6):543–551.
- Ostrovski G, Dabney W, Munos R (2018) Autoregressive quantile networks for generative modeling. *Proceedings of the 35th International Conference on Machine Learning*, 3936–3945.
- Parzen E (1960) *Modern Probability Theory and Its Applications* (Wiley-Interscience).
- Rezende D, Mohamed S (2015) Variational inference with normalizing flows. *Proceedings of the 32nd International Conference on Machine Learning*, 1530–1538.
- Saxena D, Cao J (2021) Generative adversarial networks (GANs): Challenges, solutions, and future directions. *ACM Computing Surveys* 54(3):1–42.
- Shen H, Hong LJ, Zhang X (2021) Ranking and selection with covariates for personalized decision making. *INFORMS Journal on Computing* 33(4):1500–1519.
- Sun L, Hong LJ (2010) Asymptotic representations for importance-sampling estimators of value-at-risk and conditional value-at-risk. *Operations Research Letters* 38(4):246–251.
- Torossian L, Picheny V, Faivre R, Garivier A (2020) A review on quantile regression for stochastic computer experiments. *Reliability Engineering & System Safety* 201:106858.
- van den Oord A, Kalchbrenner N, Vinyals O, Espenholt L, Graves A, Kavukcuoglu K (2016) Conditional image generation with PixelCNN decoders. *Advances in Neural Information Processing Systems* 39, 4797–4805.
- Van der Vaart AW (2000) *Asymptotic Statistics* (Cambridge university press).
- Wen R, Torkkola K (2019) Deep generative quantile-copula models for probabilistic forecasting. *arXiv preprint arXiv:1907.10697* .
- Zheng M, Li T, Zhu R, Tang Y, Tang M, Lin L, Ma Z (2020) Conditional Wasserstein generative adversarial network-gradient penalty-based approach to alleviating imbalanced data classification. *Information Sciences* 512:1009–1023.

Supplemental Material

EC.1. Extremal Quantile Regression and Lemma 5

The Bahadur representation for the extreme quantiles, i.e., Lemma 5, is crucial for our analysis of the rate of convergence. Because of its reliance on extreme value theory and involved technical details, we defer the preliminaries and assumptions of the extremal quantile regression, as well as the rigorous formulation of Lemma 5 with its proof to this section. Also, we only focus on the results on the right tail, while the results on the left tail can be obtained similarly.

We first introduce the necessary preliminaries on extremal quantile regression. It should be noted that there is a slight deviation from our setting, Chernozhukov (2005) regards \mathbf{x} as a realization of a random vector \mathbf{X} , rather than given covariates. Nevertheless, these results can be readily adapted. For technical reasons, we maintain the framework of Chernozhukov (2005).

For a random variable u , whose survival function is \tilde{F}_u , with upper endpoint $s_u = \infty$ or $s_u = 0$. According to Resnick (2008), we say that \tilde{F}_u has right tails of type 1,2 or 3 if for

$$\begin{aligned} \text{type 1:} & \text{ as } z \rightarrow s_u = \infty \text{ or } 0, & \tilde{F}_u(z + va(z)) \sim e^v \tilde{F}_u(z) & \quad \forall v \in \mathbb{R}, \\ \text{type 2:} & \text{ as } z \rightarrow s_u = \infty, & \tilde{F}_u(vz) \sim v^{-1/\xi} \tilde{F}_u(z) & \quad \forall v > 0, \xi > 0, \\ \text{type 3:} & \text{ as } z \rightarrow s_u = 0, & \tilde{F}_u(vz) \sim v^{-1/\xi} \tilde{F}_u(z) & \quad \forall v > 0, \xi < 0, \end{aligned}$$

where $a(z) = \int_z^{s_u} \tilde{F}_u(v) dv / \tilde{F}_u(z)$ for $z < s_u$, ξ is often referred to as the extreme value index, and types 1, 2, and 3 correspond to $\xi = 0$, $\xi > 0$, and $\xi < 0$, respectively. In addition, $a(z) \sim b(z)$ indicates that the ratio of $a(z)$ and $b(z)$ approaches 1 as the specified limit is taken over z . Replacing the survival function \tilde{F}_u with distribution function F_u and using the lower endpoint $\tilde{s}_u = -\infty$ or $\tilde{s}_u = 0$ will obtain the definition of types 1, 2 and 3 for left tails, and this principle also applies to all extensions of right-tail to left-tail related results below.

After defining three types of tails, the following assumption on the tail equivalence of the conditional distribution function is required, to separate the influence of the covariates from the extreme tail behavior.

ASSUMPTION EC.1.

(4.a) *There exist an auxiliary line $\mathbf{x} \mapsto \mathbf{x}^T \boldsymbol{\beta}_r$, where $\boldsymbol{\beta}_r$ is a constant vector, and some \tilde{F}_u with type 1,2 or 3 tails, such that for U , defined as $Y - \mathbf{X}^T \boldsymbol{\beta}_r$, with $s_U = +\infty$ or $s_U = 0$, we have that its conditional survival function $\tilde{F}_U(z | \mathbf{x})$ has a product form*

$$\tilde{F}_U(z | \mathbf{x}) \sim K(\mathbf{x}) \cdot \tilde{F}_u(z) \quad \text{uniformly in } \mathbf{x} \in \mathcal{X}, \text{ as } z \rightarrow s_U,$$

where $K(\cdot) > 0$ is a continuous bounded function on \mathcal{X} . Without loss of generality, let $K(\mathbf{x}) = 1$ at $\mathbf{x} = \mu_{\mathbf{X}}$, and $\tilde{F}_u(z) = \tilde{F}_U(z | \mu_{\mathbf{X}})$, where $\mu_{\mathbf{X}}$ is the mean of \mathbf{X} .

(4.b) Let $F_{\mathbf{X}}$ denote the distribution of $\mathbf{X} = (1, \mathbf{X}_{-1}^T)^T$ and $D_0 = \mathbb{E}(\mathbf{X}\mathbf{X}^T)$. Then, $F_{\mathbf{X}}$ has a compact support \mathcal{X} and D_0 is positive definite. Without loss of generality, let $\mu_{\mathbf{X}} = (1, 0, \dots, 0)^T$.

While Assumption (4.a) seems strong, Examples 3.1 to 3.3 of Chernozhukov (2005) show that Assumption (4.a) can cover not only the conventional location shift model and location-scale shift model but more. Assumption (4.b) strengthens Assumption 3 by requiring the compactness of \mathcal{X} . Moreover, Chernozhukov (2005) proves that the specific forms of $K(\cdot)$ in Assumption (4.a) for the type 1, 2, and 3 tails are as follows: for some $\mathbf{c} \in \mathbb{R}^p$,

$$K(\mathbf{x}) = \begin{cases} e^{-\mathbf{x}^T \mathbf{c}}, & \text{when } \tilde{F}_u \text{ has type 1 tails,} \\ (\mathbf{x}^T \mathbf{c})^{1/\xi}, & \text{when } \tilde{F}_u \text{ has type 2 tails, } \xi > 0, \\ (\mathbf{x}^T \mathbf{c})^{1/\xi}, & \text{when } \tilde{F}_u \text{ has type 3 tails, } \xi < 0, \end{cases}$$

where $\mu_{\mathbf{X}}^T \mathbf{c} = 0$ for type 1 tails and $\mu_{\mathbf{X}}^T \mathbf{c} = 1$ for type 2 and 3 tails.

Let $\partial F_U^{-1}(\tau | \mathbf{x}) / \partial \tau$ denote the conditional quantile density function of U , and it is the first-order derivative of the conditional quantile function $F_U^{-1}(\tau | \mathbf{x})$ (Chernozhukov 2005). Let $\phi = 1 - \tau$. Then, $F_U^{-1}(\tau | \mathbf{x}) = \tilde{F}_U^{-1}(\phi | \mathbf{x})$ and $\partial F_U^{-1}(\tau | \mathbf{x}) / \partial \tau = -\partial \tilde{F}_U^{-1}(\phi | \mathbf{x}) / \partial \phi$. The right tail that we consider corresponds to $\tau \rightarrow 1$, which is equivalent to $\phi \rightarrow 0$. we need the following Assumption 5 on the existence and behaviors of $\partial \tilde{F}_U^{-1}(\phi | \mathbf{x}) / \partial \phi$.

ASSUMPTION EC.2. *The function $\partial \tilde{F}_U^{-1}(\phi | \mathbf{x}) / \partial \phi$ exists and it satisfies*

$$(5.a) \quad \frac{\partial \tilde{F}_U^{-1}(\phi | \mathbf{x})}{\partial \phi} \sim \frac{\partial \tilde{F}_u^{-1}(\phi / K(\mathbf{x}))}{\partial \phi} \text{ uniformly in } \mathbf{x} \in \mathcal{X} \text{ as } \phi \rightarrow 0,$$

$$(5.b) \quad \frac{\partial \tilde{F}_u^{-1}(\phi)}{\partial \phi} \text{ is regularly varying at 0 with exponent } -\xi - 1.$$

Firstly, in Assumption (5.a), we strengthen the previous Assumption (4.a) by requiring tail equivalence of the conditional quantile density functions instead of only the conditional distribution functions. Secondly, in Assumption (5.b), we require the regular variation of $\partial \tilde{F}_u^{-1}(\phi) / \partial \phi$, which is known as a von Mises type condition. For a detailed analysis on its plausibility, please refer to Dekkers and Haan (1989).

With Assumptions EC.1 and EC.2, we can now give a rigorous statement of Lemma 5 and provide its proof.

LEMMA EC.1 (**Lemma 5**). *Suppose that Assumptions 4 and 5 hold, and that $\{\mathbf{X}_i, Y_i\}$ is an i.i.d. sequence. Then, if τ satisfies $\tau \rightarrow 1$ and $(1 - \tau)n \rightarrow \infty$ as $n \rightarrow \infty$, we have*

$$\sqrt{\frac{n}{1 - \tau}} f_Y(F_Y^{-1}(\tau | \mathbf{x}^*) | \mathbf{x}^*) \cdot [\hat{\beta}(\tau) - \beta(\tau)] = D_3^{-1} \tilde{W}_n(\tau) + o_{\mathbb{P}}(1), \quad (\text{EC.1.1})$$

where $D_3^{-1} = \frac{D_H^{-1}}{H(\mathbf{x}^*)}$ and $D_H = \mathbb{E}[H(\mathbf{X})^{-1} \mathbf{X}\mathbf{X}^T]$, $H(\mathbf{x}) = 1$ for type 1 tails, $H(\mathbf{x}) = \mathbf{x}^T \mathbf{c}$ for type 2 and 3 tails, $\mathbf{c} \in \mathbb{R}^p$ is a constant vector determined by $K(\mathbf{x})$,

$$\tilde{W}_n(\tau) = \frac{1}{\sqrt{(1 - \tau)n}} \sum_{i=1}^n \mathbf{X}_i \psi_{\tau}(Y_i - \beta^T(\tau) \mathbf{X}_i), \quad (\text{EC.1.2})$$

and $\tilde{W}_n(\tau) \Rightarrow N(0, D_0)$.

Notice that here we state the lemma using the setting of Chernozhukov (2005), hence the realization (\mathbf{x}_i, y_i) is replaced by the random vector (\mathbf{X}_i, Y_i) , and D_0 represents $\mathbb{E}(\mathbf{X}\mathbf{X}^\top)$ in their setting, while, by the law of large numbers, it is the same as D_0 in our setting, which is $\lim_{n \rightarrow \infty} \frac{1}{n} \sum_{i=1}^n \mathbf{x}_i \mathbf{x}_i^\top$.

Proof of Lemma EC.1 (Lemma 5). First, Equation (EC.1.2) and the convergence of $\tilde{W}_n(\tau)$ to $N(0, D_0)$ are direct extensions of Lemma 9.6 of Chernozhukov (2005) for the right tail (notice that the minus sign can be neglected as $N(0, D_0)$ is symmetric to 0). Furthermore, following the Step 1 of the proof of Theorem 5.1 of Chernozhukov (2005), for the right tail, we have

$$\frac{\sqrt{(1-\tau)n} \left(\hat{\boldsymbol{\beta}}(\tau) - \boldsymbol{\beta}(\tau) \right)}{\mu_{\mathbf{X}}^\top \boldsymbol{\beta}(1-k(1-\tau)) - \mu_{\mathbf{X}}^\top \boldsymbol{\beta}(\tau)} = \frac{-\xi}{k^{-\xi} - 1} \frac{D_H^{-1}}{\sqrt{(1-\tau)n}} \sum_{i=1}^n \mathbf{X}_i \psi_\tau(Y_i - \boldsymbol{\beta}(\tau)^\top \mathbf{X}_i) + o_{\mathbb{P}}(1). \quad (\text{EC.1.3})$$

Moreover, the relationships (9.61) to (9.65) of Chernozhukov (2005) can be similarly derived for the right tail, which states that

$$\lim_{\tau \rightarrow 1} \frac{\tilde{F}_u^{-1}(k(1-\tau)) - \tilde{F}_u^{-1}(1-\tau)}{(1-\tau) (f_Y(F_Y^{-1}(\tau|\mathbf{x}^*)|\mathbf{x}^*))^{-1}} = \frac{1}{H(\mathbf{x}^*)} \cdot \frac{k^{-\xi} - 1}{-\xi}.$$

With this relationship, and notice that

$$\begin{aligned} \frac{\mu_{\mathbf{X}}^\top \boldsymbol{\beta}(1-k(1-\tau)) - \mu_{\mathbf{X}}^\top \boldsymbol{\beta}(\tau)}{(1-\tau) (f_Y(F_Y^{-1}(\tau|\mathbf{x}^*)|\mathbf{x}^*))^{-1}} &= \frac{(\mu_{\mathbf{X}}^\top \boldsymbol{\beta}(1-k(1-\tau)) - \mu_{\mathbf{X}}^\top \boldsymbol{\beta}_r) - (\mu_{\mathbf{X}}^\top \boldsymbol{\beta}(\tau) - \mu_{\mathbf{X}}^\top \boldsymbol{\beta}_r)}{(1-\tau) (f_Y(F_Y^{-1}(\tau|\mathbf{x}^*)|\mathbf{x}^*))^{-1}} \\ &= \frac{\tilde{F}_u^{-1}(k(1-\tau)) - \tilde{F}_u^{-1}(1-\tau)}{(1-\tau) (f_Y(F_Y^{-1}(\tau|\mathbf{x}^*)|\mathbf{x}^*))^{-1}}, \end{aligned}$$

we can finally rewrite (EC.1.3) as (EC.1.1), which completes the proof. \square

EC.2. Additional Proofs

EC.2.1. Proof of Proposition 2

Notice that for any given subinterval $[\tau_\ell, \tau_u] \subset (0, 1)$ with $0 < \tau_\ell < \tau_u < 1$ and any given m , since τ_ℓ and τ_u are not required to be symmetric, there are three cases for the relation between $[\tau_\ell, \tau_u]$ and $[\frac{1}{m}, 1 - \frac{1}{m}]$, that is, $[\frac{1}{m}, 1 - \frac{1}{m}] \subset [\tau_\ell, \tau_u]$, $[\tau_\ell, \tau_u] \subseteq [\frac{1}{m}, 1 - \frac{1}{m}]$, and $[\tau_\ell, \tau_u]$ intersects with $[\frac{1}{m}, 1 - \frac{1}{m}]$. We prove Proposition 2 for each of these three cases, respectively.

Case 1: $[\frac{1}{m}, 1 - \frac{1}{m}] \subset [\tau_\ell, \tau_u]$.

For $\tau \in [\tau_\ell, \tau_1)$, we have $\tilde{\boldsymbol{\beta}}(\tau) = \hat{\boldsymbol{\beta}}_1$. Write

$$\tilde{\boldsymbol{\beta}}(\tau) - \boldsymbol{\beta}(\tau) = \hat{\boldsymbol{\beta}}_1 - \boldsymbol{\beta}(\tau) = \hat{\boldsymbol{\beta}}_1 - \boldsymbol{\beta}(\tau_1) + \boldsymbol{\beta}(\tau_1) - \boldsymbol{\beta}(\tau).$$

For $\tau \in [\tau_j, \tau_{j+1})$, denote $\frac{\tau_{j+1} - \tau}{\tau_{j+1} - \tau_j}$ as α , then we have $\tilde{\boldsymbol{\beta}}(\tau) = \alpha \hat{\boldsymbol{\beta}}_j + (1 - \alpha) \hat{\boldsymbol{\beta}}_{j+1}$. Write

$$\begin{aligned} &\tilde{\boldsymbol{\beta}}(\tau) - \boldsymbol{\beta}(\tau) \\ &= \alpha \left(\hat{\boldsymbol{\beta}}_j - \boldsymbol{\beta}(\tau_j) \right) + (1 - \alpha) \left(\hat{\boldsymbol{\beta}}_{j+1} - \boldsymbol{\beta}(\tau_{j+1}) \right) + \alpha (\boldsymbol{\beta}(\tau_j) - \boldsymbol{\beta}(\tau)) + (1 - \alpha) (\boldsymbol{\beta}(\tau_{j+1}) - \boldsymbol{\beta}(\tau)). \end{aligned}$$

For $\tau \in [\tau_{m-1}, \tau_u]$, we have $\tilde{\beta}(\tau) = \hat{\beta}_{m-1}$. Write

$$\tilde{\beta}(\tau) - \beta(\tau) = \hat{\beta}_{m-1} - \beta(\tau) = \hat{\beta}_{m-1} - \beta(\tau_{m-1}) + \beta(\tau_{m-1}) - \beta(\tau).$$

Thus, recall that $F_Y^{-1}(\tau|\mathbf{x}^*) = \beta(\tau)\mathbf{x}^*$, we then have

$$\begin{aligned} & \sup_{\tau \in [\tau_\ell, \tau_u]} \left| \hat{Y}(\tau|\mathbf{x}^*) - F_Y^{-1}(\tau|\mathbf{x}^*) \right| \\ & \leq \max_{\substack{\tau_j \in [\tau_\ell, \tau_u] \\ 1 \leq j \leq m-1}} \|\hat{\beta}_j - \beta(\tau_j)\| \cdot \|\mathbf{x}^*\| + \sup \left\{ \sup_{\tau \in [\tau_\ell, \tau_1]} |F_Y^{-1}(\tau_1|\mathbf{x}^*) - F_Y^{-1}(\tau|\mathbf{x}^*)|, \right. \\ & \quad \left. \sup_{\substack{\tau \in [\tau_{j-1}, \tau_{j+1}] \\ 2 \leq j \leq m-2}} |F_Y^{-1}(\tau|\mathbf{x}^*) - F_Y^{-1}(\tau_j|\mathbf{x}^*)|, \sup_{\tau \in [\tau_{m-1}, \tau_u]} |F_Y^{-1}(\tau|\mathbf{x}^*) - F_Y^{-1}(\tau_{m-1}|\mathbf{x}^*)| \right\} \\ & \leq \max_{\substack{\tau_j \in [\tau_\ell, \tau_u] \\ 1 \leq j \leq m-1}} \|\hat{\beta}_j - \beta(\tau_j)\| \cdot \|\mathbf{x}^*\| + \sup \left\{ |F_Y^{-1}(\tau_1|\mathbf{x}^*) - F_Y^{-1}(\tau_\ell|\mathbf{x}^*)|, \right. \\ & \quad \left. \sup_{1 \leq j \leq m-2} |F_Y^{-1}(\tau_j|\mathbf{x}^*) - F_Y^{-1}(\tau_{j+1}|\mathbf{x}^*)|, |F_Y^{-1}(\tau_u|\mathbf{x}^*) - F_Y^{-1}(\tau_{m-1}|\mathbf{x}^*)| \right\} \\ & \leq \max_{\substack{\tau_j \in [\tau_\ell, \tau_u] \\ 1 \leq j \leq m-1}} \|\hat{\beta}_j - \beta(\tau_j)\| \cdot \|\mathbf{x}^*\| + \frac{1}{m} \left(\inf_{\tau \in [\tau_\ell, \tau_u]} f_Y(F_Y^{-1}(\tau|\mathbf{x}^*)|\mathbf{x}^*) \right)^{-1}, \end{aligned}$$

where the last inequality is due to Assumption (2.b), the mean value theorem, and for any $\tau \in [\tau_\ell, \tau_u]$,

$$(F_Y^{-1}(\tau|\mathbf{x}^*))' = (f_Y(F_Y^{-1}(\tau|\mathbf{x}^*)))^{-1} \leq \left(\inf_{\tau \in [\tau_\ell, \tau_u]} f_Y(F_Y^{-1}(\tau|\mathbf{x}^*)) \right)^{-1}.$$

Case 2: $[\tau_\ell, \tau_u] \subseteq [\frac{1}{m}, 1 - \frac{1}{m}]$.

Compared with Case 1, this case is more tricky because of the problem caused by the two-side small intervals near the two endpoints τ_ℓ and τ_u , (e.g. $[\tau_j, \tau_u]$, if $\tau_u \in [\tau_j, \tau_{j+1}]$ for some j), where $\tilde{\beta}(\tau)$ are interpolated by $\hat{\beta}_j$ and $\hat{\beta}_{j+1}$, however, $\hat{\beta}_{j+1}$ is outside $[\tau_\ell, \tau_u]$, we can't ensure its uniform convergence by Proposition 1. To solve this problem, we compress each end of the interval $[\tau_\ell, \tau_u]$ inward by $\frac{1}{m}$, that is, we only consider the interval $[\tau_\ell + \frac{1}{m}, \tau_u - \frac{1}{m}]$, and it will converge to (τ_ℓ, τ_u) as $m \rightarrow \infty$.

Then, notice that for any $\tau \in [\tau_\ell + \frac{1}{m}, \tau_u - \frac{1}{m}]$, we can now always find $[\tau_j, \tau_{j+1})$ subject to $\tau \in [\tau_j, \tau_{j+1}) \subseteq [\tau_\ell, \tau_u]$. Again, write

$$\begin{aligned} & \tilde{\beta}(\tau) - \beta(\tau) \\ & = \alpha \left(\hat{\beta}_j - \beta(\tau_j) \right) + (1 - \alpha) \left(\hat{\beta}_{j+1} - \beta(\tau_{j+1}) \right) + \alpha \left(\beta(\tau_j) - \beta(\tau) \right) + (1 - \alpha) \left(\beta(\tau_{j+1}) - \beta(\tau) \right). \end{aligned}$$

Then, we have

$$\sup_{\tau \in [\tau_\ell + \frac{1}{m}, \tau_u - \frac{1}{m}]} \left| \hat{Y}(\tau|\mathbf{x}^*) - F_Y^{-1}(\tau|\mathbf{x}^*) \right|$$

$$\begin{aligned}
&\leq \max_{\substack{\tau_j \in [\tau_\ell, \tau_u] \\ 1 \leq j \leq m-1}} \|\hat{\beta}_j - \beta(\tau_j)\| \cdot \|\mathbf{x}^*\| + \sup \left\{ \sup_{\substack{\tau \in [\tau_j, \tau_{j+1}] \subseteq [\tau_\ell, \tau_u] \\ 1 \leq j \leq m-1}} |F_Y^{-1}(\tau_j | \mathbf{x}^*) - F_Y^{-1}(\tau | \mathbf{x}^*)|, \right. \\
&\quad \left. \sup_{\substack{\tau \in [\tau_j, \tau_{j+1}] \subseteq [\tau_\ell, \tau_u] \\ 1 \leq j \leq m-1}} |F_Y^{-1}(\tau_{j+1} | \mathbf{x}^*) - F_Y^{-1}(\tau | \mathbf{x}^*)| \right\} \\
&\leq \max_{\substack{\tau_j \in [\tau_\ell, \tau_u] \\ 1 \leq j \leq m-1}} \|\hat{\beta}_j - \beta(\tau_j)\| \cdot \|\mathbf{x}^*\| + \sup_{\substack{\tau_j \in [\tau_\ell, \tau_u] \\ 1 \leq j \leq m-1}} |F_Y^{-1}(\tau_{j+1} | \mathbf{x}^*) - F_Y^{-1}(\tau_j | \mathbf{x}^*)| \\
&\leq \max_{\substack{\tau_j \in [\tau_\ell, \tau_u] \\ 1 \leq j \leq m-1}} \|\hat{\beta}_j - \beta(\tau_j)\| \cdot \|\mathbf{x}^*\| + \frac{1}{m} \left(\inf_{\tau \in [\tau_\ell, \tau_u]} f_Y(F_Y^{-1}(\tau | \mathbf{x}^*) | \mathbf{x}^*) \right)^{-1}.
\end{aligned}$$

Case 3: $[\tau_\ell, \tau_u]$ intersects with $[\frac{1}{m}, 1 - \frac{1}{m}]$.

This case is just a combination of Case 1 and Case 2. Following a similar proof, we can still have

$$\begin{aligned}
&\sup_{\tau \in [\tau_\ell + \frac{1}{m}, \tau_u - \frac{1}{m}]} \left| \hat{Y}(\tau | \mathbf{x}^*) - F_Y^{-1}(\tau | \mathbf{x}^*) \right| \\
&\leq \max_{\substack{\tau_j \in [\tau_\ell, \tau_u] \\ 1 \leq j \leq m-1}} \|\hat{\beta}_j - \beta(\tau_j)\| \cdot \|\mathbf{x}^*\| + \frac{1}{m} \left(\inf_{\tau \in [\tau_\ell, \tau_u]} f_Y(F_Y^{-1}(\tau | \mathbf{x}^*) | \mathbf{x}^*) \right)^{-1}. \quad (\text{EC.2.1})
\end{aligned}$$

Thus, whichever case it is, we all have (EC.2.1). Hence, as $n, m \rightarrow \infty$, by Proposition 1, we have

$$\sup_{\tau \in (\tau_\ell, \tau_u)} \left| \hat{Y}(\tau | \mathbf{x}^*) - F_Y^{-1}(\tau | \mathbf{x}^*) \right| \xrightarrow{\mathbb{P}} 0.$$

This concludes the proof of the proposition. \square

EC.2.2. Proof of Theorem 1

We prove the convergence in distribution of $Y(\mathbf{x}^*)$ by Lemma 2. Suppose h is any given bounded, Lipschitz continuous function on \mathcal{Y} such that there exist positive constants M_h and L_h that, $|h(y)| \leq M_h$, for all $y \in \mathcal{Y}$, and $|h(y_1) - h(y_2)| \leq L_h |y_1 - y_2|$, for all $y_1, y_2 \in \mathcal{Y}$. Then, it is sufficient to show that as $n, m \rightarrow \infty$,

$$\mathbb{E}h(\hat{Y}(U | \mathbf{x}^*)) \rightarrow \mathbb{E}h(F_Y^{-1}(U | \mathbf{x}^*)),$$

where the distribution of $F_Y^{-1}(U | \mathbf{x}^*)$ given \mathbf{x}^* is the conditional distribution $F_Y(\cdot | \mathbf{x}^*)$.

For any given $\varepsilon_1 > 0$, by Lemma 4, given $\tau_\ell = \frac{\varepsilon_1}{10(M_h \vee 1)}$, $\tau_u = 1 - \frac{\varepsilon_1}{10(M_h \vee 1)}$, for any $\varepsilon_2 > 0$, there exist sufficiently large $N(\varepsilon_1, \varepsilon_2), M(\varepsilon_1, \varepsilon_2)$, such that for any $n \geq N(\varepsilon_1, \varepsilon_2)$, $m \geq M(\varepsilon_1, \varepsilon_2)$, we have

$$\mathbb{E} \left[\left| h(\hat{Y}(U | \mathbf{x}^*)) - h(F_Y^{-1}(U | \mathbf{x}^*)) \right| \mathbb{I}\{U \in I_3\} \right] \leq \frac{\varepsilon_2}{5}. \quad (\text{EC.2.2})$$

Then, take sufficiently large $M'(\varepsilon_1, \varepsilon_2) = M(\varepsilon_1, \varepsilon_2) \vee \frac{10(M_h \vee 1)}{\varepsilon_1}$ such that for any $n \geq N(\varepsilon_1, \varepsilon_2)$, $m \geq M'(\varepsilon_1, \varepsilon_2)$, we have that $\frac{1}{m} \leq \frac{\varepsilon_1}{10(M_h \vee 1)}$ and (EC.2.2). Notice that by the analysis of Proposition 2, (EC.2.2) keeps valid no matter what relationship between $[\tau_\ell, \tau_u]$ and $[\frac{1}{m}, 1 - \frac{1}{m}]$ is.

Since (EC.2.2) is satisfied for any $\varepsilon_1, \varepsilon_2 > 0$, let $\varepsilon_2 = \varepsilon_1$, then we have the following statement: for any given bounded Lipschitz continuous function h , any $\varepsilon_1 > 0$, $\tau_\ell = \frac{\varepsilon_1}{10(M_h \vee 1)}$, and $\tau_u = 1 - \frac{\varepsilon_1}{10(M_h \vee 1)}$, there exist sufficiently large $N = N(\varepsilon_1, \varepsilon_1)$, $M' = M'(\varepsilon_1, \varepsilon_1)$, such that for any $n \geq N$, $m \geq M'$, we have that $\frac{1}{m} \leq \frac{\varepsilon_1}{10(M_h \vee 1)}$ and (EC.2.2).

Hence, it is straightforward to see

$$\begin{aligned} & \left| \mathbb{E}h(\hat{Y}(U|\mathbf{x}^*)) - \mathbb{E}h(F_Y^{-1}(U|\mathbf{x}^*)) \right| \\ & \leq \mathbb{E} \left[\left| \left(h(\hat{Y}(U|\mathbf{x}^*)) - h(F_Y^{-1}(U|\mathbf{x}^*)) \right) \right| \mathbb{I}\{U \in I_1\} \right] + \mathbb{E} \left[\left| \left(h(\hat{Y}(U|\mathbf{x}^*)) - h(F_Y^{-1}(U|\mathbf{x}^*)) \right) \right| \mathbb{I}\{U \in I_2\} \right] \\ & + \mathbb{E} \left[\left| \left(h(\hat{Y}(U|\mathbf{x}^*)) - h(F_Y^{-1}(U|\mathbf{x}^*)) \right) \right| \mathbb{I}\{U \in I_3\} \right] + \mathbb{E} \left[\left| \left(h(\hat{Y}(U|\mathbf{x}^*)) - h(F_Y^{-1}(U|\mathbf{x}^*)) \right) \right| \mathbb{I}\{U \in I_4\} \right] \\ & + \mathbb{E} \left[\left| \left(h(\hat{Y}(U|\mathbf{x}^*)) - h(F_Y^{-1}(U|\mathbf{x}^*)) \right) \right| \mathbb{I}\{U \in I_5\} \right] \\ & \leq \frac{8M_h \cdot \varepsilon_1}{10(M_h \vee 1)} + \frac{\varepsilon_1}{5} \leq \varepsilon_1, \end{aligned}$$

which completes the proof. \square

EC.2.3. Proof of Example 1

We intend to verify Assumptions 4 and 5 to derive the asymptotic result of the intermediate quantile regression by Lemma EC.1. We first validate the case that F_0 is the uniform distribution in $[0, 1]$. Notice that it can be seen as having the tail of type 3 with $\xi = -1$ (An easier way to validate this is to consider the left tails by definition and notice that the uniform distribution has symmetric tail behaviors). In addition, under the location shift model (12), whether tails are type 1, 2, or 3, we all have $\beta_r = \beta$, $K(\mathbf{x}) = 1$ and $H(\mathbf{x}) = 1$ by example 3.1 and remark 3.2 of Chernozhukov (2005). And for the uniform distribution in $[0, 1]$, $\tilde{F}_U(z|\mathbf{x}) = \tilde{F}_u(z) = \tilde{F}_0(z) = 1 - z$ for $z \in [0, 1]$, and $\tilde{F}_U^{-1}(\phi|\mathbf{x}) = \tilde{F}_u^{-1}(\phi) = 1 - \phi = \tau$ for $\phi \in [0, 1]$.

To make it clearer, we restate the Assumptions 4 and 5 and verify them under the current case.

(4.a) Given the survival distributions $\tilde{F}_U(z|\mathbf{x}) = 1 - z = \tilde{F}_u(z)$, it holds that

$$\lim_{z \rightarrow \infty} \frac{\tilde{F}_U(z|\mathbf{x})}{\tilde{F}_u(z)K(\mathbf{x})} = 1$$

uniformly for all \mathbf{x} with $K(\mathbf{x}) = 1$ for all $\mathbf{x} \in \mathcal{X}$.

(4.b) The predictor \mathbf{X} has compact support \mathcal{X} with $\mathbb{E}(\mathbf{X}\mathbf{X}^\top)$ positive definite.

(5.c) Uniformly for all \mathbf{x} ,

$$\lim_{\phi \rightarrow 0} \frac{\partial \tilde{F}_U^{-1}(\phi|\mathbf{x}) / \partial \phi}{\partial \tilde{F}_u^{-1}(\phi/K(\mathbf{x})) / \partial \phi} = 1.$$

(5.d) For any $t > 0$,

$$\lim_{\phi \rightarrow 0} \frac{\left(\partial \tilde{F}_u^{-1}(p) / \partial p \right) \Big|_{p=t\phi}}{\left(\partial \tilde{F}_u^{-1}(p) / \partial p \right) \Big|_{p=\phi}} = 1 = t^0,$$

which corresponds to $\xi = -1$.

Hence, by Lemma EC.1, we can derive (13).

For the case of the exponential distribution and Pareto distribution, the proofs are similar, except for the exponential distribution, $\tilde{F}_0(z) = e^{-\lambda z}$ for $z \geq 0$, $\tilde{F}_0^{-1}(\phi) = -\frac{\ln(\phi)}{\lambda}$ and $f_0(F_0^{-1}(1 - \frac{1}{m})) = \frac{\lambda}{m}$, and for **(5.d)**, for any $t > 0$, we have

$$\lim_{\phi \rightarrow 0} \frac{\left(\frac{\partial \tilde{F}_u^{-1}(p)}{\partial \phi}\right) \Big|_{p=t\phi}}{\left(\frac{\partial \tilde{F}_u^{-1}(p)}{\partial \phi}\right) \Big|_{p=\phi}} = t^{-1},$$

which corresponds to the requirement of **(5.d)** with $\xi = 0$, and the exponential distribution exactly has the tail of type 1 with $\xi = 0$; and for Pareto distribution, $\tilde{F}_0(z) = z^{-\gamma}$, $\tilde{F}_0^{-1}(\phi) = \phi^{-1/\gamma}$ and $f_0(F_0^{-1}(1 - \frac{1}{m})) = \gamma(\frac{1}{m})^{1+1/\gamma}$, and for **(5.d)**, for any $t > 0$, we have

$$\lim_{\phi \rightarrow 0} \frac{\left(\frac{\partial F_u^{-1}(p)}{\partial \phi}\right) \Big|_{p=t\phi}}{\left(\frac{\partial F_u^{-1}(p)}{\partial \phi}\right) \Big|_{p=\phi}} = t^{-1/\gamma-1},$$

which corresponds to the requirement of **(5.d)** with $\xi = \frac{1}{\gamma}$, and Pareto distribution exactly has the tail of type 2 with $\xi = \frac{1}{\gamma}$. \square

EC.2.4. Proof of Lemma 6

First, since QRGMM truncates $\hat{Y}(\tau|\mathbf{x}^*)$ at τ_1 and τ_{m-1} , we can break $\sup_{y \in (-\infty, \infty)} |F_{\hat{Y}}(y|\mathbf{x}^*) - F_Y(y|\mathbf{x}^*)|$ into three parts:

$$\begin{aligned} & \sup_{y \in (-\infty, \infty)} |F_{\hat{Y}}(y|\mathbf{x}^*) - F_Y(y|\mathbf{x}^*)| \\ &= \sup \left\{ \begin{aligned} & \sup_{y \in (-\infty, \hat{Y}(\tau_1|\mathbf{x}^*))} |F_{\hat{Y}}(y|\mathbf{x}^*) - F_Y(y|\mathbf{x}^*)|, \quad \sup_{y \in (\hat{Y}(\tau_{m-1}|\mathbf{x}^*), \infty)} |F_{\hat{Y}}(y|\mathbf{x}^*) - F_Y(y|\mathbf{x}^*)|, \\ & \sup_{y \in [\hat{Y}(\tau_1|\mathbf{x}^*), \hat{Y}(\tau_{m-1}|\mathbf{x}^*)]} |F_{\hat{Y}}(y|\mathbf{x}^*) - F_Y(y|\mathbf{x}^*)| \end{aligned} \right\} \\ &= \sup \left\{ \begin{aligned} & \sup_{y \in (-\infty, \hat{Y}(\tau_1|\mathbf{x}^*))} |0 - F_Y(y|\mathbf{x}^*)|, \quad \sup_{y \in (\hat{Y}(\tau_{m-1}|\mathbf{x}^*), \infty)} |1 - F_Y(y|\mathbf{x}^*)| \\ & \sup_{y \in [\hat{Y}(\tau_1|\mathbf{x}^*), \hat{Y}(\tau_{m-1}|\mathbf{x}^*)]} |F_{\hat{Y}}(y|\mathbf{x}^*) - F_Y(y|\mathbf{x}^*)|, \end{aligned} \right\} \tag{EC.2.3} \\ &= \sup \left\{ \begin{aligned} & F_Y(\hat{Y}(\tau_1|\mathbf{x}^*)|\mathbf{x}^*), 1 - F_Y(\hat{Y}(\tau_{m-1}|\mathbf{x}^*)|\mathbf{x}^*), \quad \sup_{y \in [\hat{Y}(\tau_1|\mathbf{x}^*), \hat{Y}(\tau_{m-1}|\mathbf{x}^*)]} |F_{\hat{Y}}(y|\mathbf{x}^*) - F_Y(y|\mathbf{x}^*)| \end{aligned} \right\} \\ &= \sup \left\{ \begin{aligned} & F_Y(\hat{Y}(\tau_1|\mathbf{x}^*)|\mathbf{x}^*), 1 - F_Y(\hat{Y}(\tau_{m-1}|\mathbf{x}^*)|\mathbf{x}^*), \quad \sup_{\tau \in [\tau_1, \tau_{m-1}]} \left| F_{\hat{Y}}(\hat{Y}(\tau|\mathbf{x}^*)|\mathbf{x}^*) - F_Y(\hat{Y}(\tau|\mathbf{x}^*)|\mathbf{x}^*) \right| \end{aligned} \right\} \\ &= \sup \left\{ F_Y(\hat{Y}(\tau_1|\mathbf{x}^*)|\mathbf{x}^*) - \tau_1 + \frac{1}{m}, \tau_{m-1} - F_Y(\hat{Y}(\tau_{m-1}|\mathbf{x}^*)|\mathbf{x}^*) + \frac{1}{m}, \right\} \end{aligned}$$

$$\sup_{\tau \in [\tau_1, \tau_{m-1}]} \left| F_{\hat{Y}}(\hat{Y}(\tau|\mathbf{x}^*)|\mathbf{x}^*) - F_Y(\hat{Y}(\tau|\mathbf{x}^*)|\mathbf{x}^*) \right|. \quad (\text{EC.2.4})$$

Equation (EC.2.3) is derived from the fact that $F_{\hat{Y}}(y|\mathbf{x}^*)$ takes the values of 0 and 1 on the intervals $(-\infty, \hat{Y}(\tau_1|\mathbf{x}^*))$ and $(\hat{Y}(\tau_{m-1}|\mathbf{x}^*), \infty)$ respectively due to the truncation of $\hat{Y}(\tau|\mathbf{x}^*)$. The equation preceding equation (EC.2.3) arises from the fact that $\hat{Y}(\tau|\mathbf{x}^*)$ is a piecewise linear and therefore continuous function of τ , and there is a one-to-one relationship between $\hat{Y}(\tau|\mathbf{x}^*)$ and τ within $[\hat{Y}(\tau_1|\mathbf{x}^*), \hat{Y}(\tau_{m-1}|\mathbf{x}^*)]$. Thus, we can replace $y \in [\hat{Y}(\tau_1|\mathbf{x}^*), \hat{Y}(\tau_{m-1}|\mathbf{x}^*)]$ with $\hat{Y}(\tau|\mathbf{x}^*)$ where $\tau \in [\tau_1, \tau_{m-1}]$.

The last term on the right side of the equation (EC.2.4) can be further decomposed. Notice that for $\tau \in [\tau_j, \tau_{j+1}] \subseteq [\tau_1, \tau_{m-1}]$, if we denote $\tilde{\alpha} = \frac{\hat{Y}(\tau_{j+1}|\mathbf{x}^*) - \hat{Y}(\tau|\mathbf{x}^*)}{\hat{Y}(\tau_{j+1}|\mathbf{x}^*) - \hat{Y}(\tau_j|\mathbf{x}^*)}$, then $1 - \tilde{\alpha} = \frac{\hat{Y}(\tau|\mathbf{x}^*) - \hat{Y}(\tau_j|\mathbf{x}^*)}{\hat{Y}(\tau_{j+1}|\mathbf{x}^*) - \hat{Y}(\tau_j|\mathbf{x}^*)}$. Since $F_{\hat{Y}}(\hat{Y}(\tau|\mathbf{x}^*)|\mathbf{x}^*)$ is linearly interpolated between $F_{\hat{Y}}(\hat{Y}(\tau_j|\mathbf{x}^*)|\mathbf{x}^*)$ and $F_{\hat{Y}}(\hat{Y}(\tau_{j+1}|\mathbf{x}^*)|\mathbf{x}^*)$, we have

$$\begin{aligned} & F_{\hat{Y}}(\hat{Y}(\tau|\mathbf{x}^*)|\mathbf{x}^*) - F_Y(\hat{Y}(\tau|\mathbf{x}^*)|\mathbf{x}^*) \\ &= \tilde{\alpha} \left(F_{\hat{Y}}(\hat{Y}(\tau_j|\mathbf{x}^*)|\mathbf{x}^*) - F_Y(\hat{Y}(\tau_j|\mathbf{x}^*)|\mathbf{x}^*) \right) + (1 - \tilde{\alpha}) \left(F_{\hat{Y}}(\hat{Y}(\tau_{j+1}|\mathbf{x}^*)|\mathbf{x}^*) - F_Y(\hat{Y}(\tau_{j+1}|\mathbf{x}^*)|\mathbf{x}^*) \right) \\ &+ \tilde{\alpha} \left(F_Y(\hat{Y}(\tau_j|\mathbf{x}^*)|\mathbf{x}^*) - F_Y(\hat{Y}(\tau|\mathbf{x}^*)|\mathbf{x}^*) \right) + (1 - \tilde{\alpha}) \left(F_Y(\hat{Y}(\tau_{j+1}|\mathbf{x}^*)|\mathbf{x}^*) - F_Y(\hat{Y}(\tau|\mathbf{x}^*)|\mathbf{x}^*) \right) \\ &= \tilde{\alpha} \left(\tau_j - F_Y(\hat{Y}(\tau_j|\mathbf{x}^*)|\mathbf{x}^*) \right) + (1 - \tilde{\alpha}) \left(\tau_{j+1} - F_Y(\hat{Y}(\tau_{j+1}|\mathbf{x}^*)|\mathbf{x}^*) \right) \\ &+ \tilde{\alpha} \left(F_Y(\hat{Y}(\tau_j|\mathbf{x}^*)|\mathbf{x}^*) - F_Y(\hat{Y}(\tau|\mathbf{x}^*)|\mathbf{x}^*) \right) + (1 - \tilde{\alpha}) \left(F_Y(\hat{Y}(\tau_{j+1}|\mathbf{x}^*)|\mathbf{x}^*) - F_Y(\hat{Y}(\tau|\mathbf{x}^*)|\mathbf{x}^*) \right). \end{aligned}$$

In the right-hand side of the last equation, the first two items stand for the estimation errors of the cumulative distribution functions, and the last two items stand for the interpolation errors of the cumulative distribution functions. However, as the following equation shows, the bound of the interpolation errors of the cumulative distribution functions can be further decomposed as the sum of the estimation errors of the cumulative distribution functions and $\frac{1}{m}$:

$$\begin{aligned} & F_Y(\hat{Y}(\tau_{j+1}|\mathbf{x}^*)|\mathbf{x}^*) - F_Y(\hat{Y}(\tau_j|\mathbf{x}^*)|\mathbf{x}^*) \\ &= F_Y(\hat{Y}(\tau_{j+1}|\mathbf{x}^*)|\mathbf{x}^*) - \tau_{j+1} + \tau_{j+1} - \tau_j + \tau_j - F_Y(\hat{Y}(\tau_j|\mathbf{x}^*)|\mathbf{x}^*) \\ &= \left(F_Y(\hat{Y}(\tau_{j+1}|\mathbf{x}^*)|\mathbf{x}^*) - \tau_{j+1} \right) + \frac{1}{m} + \left(\tau_j - F_Y(\hat{Y}(\tau_j|\mathbf{x}^*)|\mathbf{x}^*) \right). \end{aligned}$$

Therefore, we have

$$\sup_{y \in (-\infty, \infty)} |F_{\hat{Y}}(y|\mathbf{x}^*) - F_Y(y|\mathbf{x}^*)| \leq 3 \max_{1 \leq j \leq m-1} \left| \tau_j - F_Y(\hat{Y}(\tau_j|\mathbf{x}^*)|\mathbf{x}^*) \right| + \frac{1}{m}.$$

This completes the proof of the lemma. \square

EC.2.5. Proof of Theorem 2

Lemma 6 shows that the maximum error of $F_{\hat{Y}}(y|\mathbf{x}^*)$ is dominated by the sum of the maximum estimation error of $F_Y(\hat{Y}(\tau|\mathbf{x}^*)|\mathbf{x}^*)$ at interpolation points and the interpolation length $\frac{1}{m}$. Consequently, we only need to investigate the the maximum estimation error of $F_Y(\hat{Y}(\tau|\mathbf{x}^*)|\mathbf{x}^*)$.

For a given m and n , define

$$j_{m,n}^* = \arg \max_{1 \leq j \leq m-1} \left| \tau_j - F_Y(\hat{Y}(\tau_j|\mathbf{x}^*)|\mathbf{x}^*) \right|, \quad (\text{EC.2.5})$$

then $\tau_{j_{m,n}^*}$ can be seen as a sequence associated with m and n , such that

$$\left| \tau_{j_{m,n}^*} - F_Y(\hat{Y}(\tau_{j_{m,n}^*}|\mathbf{x}^*)|\mathbf{x}^*) \right| = \max_{1 \leq j \leq m-1} \left| \tau_j - F_Y(\hat{Y}(\tau_j|\mathbf{x}^*)|\mathbf{x}^*) \right|.$$

Therefore, by Lemma 6, to derive the uniform rate of convergence of $F_{\hat{Y}}(y|\mathbf{x}^*)$, we only need to find the rate of convergence of $F_Y(\hat{Y}(\tau_{j_{m,n}^*}|\mathbf{x}^*)|\mathbf{x}^*)$.

For the sequence $\tau_{j_{m,n}^*}$, we first consider its three special but important possible cases separately:

Case 1 $\tau_{j_{m,n}^*} \rightarrow 0$ as $m, n \rightarrow \infty$;

Case 2 $\tau_{j_{m,n}^*} \rightarrow 1$ as $m, n \rightarrow \infty$;

Case 3 there exist $\varepsilon_1 > 0$ and $\varepsilon_2 > 0$, such that $\tau_{j_{m,n}^*} \in [\varepsilon_1, 1 - \varepsilon_2]$ when m, n are sufficiently large,

let $\tau_\ell = \varepsilon_1$ and $\tau_u = 1 - \varepsilon_2$.

For the above three cases, we will prove the following results:

- For Case 1,

$$\left| \tau_{j_{m,n}^*} - F_Y(\hat{Y}(\tau_{j_{m,n}^*}|\mathbf{x}^*)|\mathbf{x}^*) \right| = O_{\mathbb{P}} \left(\frac{\sqrt{\tau_{j_{m,n}^*}}}{\sqrt{n}} \right) \quad (\text{EC.2.6})$$

as $m, n \rightarrow \infty$.

- For Case 2,

$$\left| \tau_{j_{m,n}^*} - F_Y(\hat{Y}(\tau_{j_{m,n}^*}|\mathbf{x}^*)|\mathbf{x}^*) \right| = O_{\mathbb{P}} \left(\frac{\sqrt{1 - \tau_{j_{m,n}^*}}}{\sqrt{n}} \right) \quad (\text{EC.2.7})$$

as $m, n \rightarrow \infty$.

- For Case 3,

$$\left| \tau_{j_{m,n}^*} - F_Y(\hat{Y}(\tau_{j_{m,n}^*}|\mathbf{x}^*)|\mathbf{x}^*) \right| = O_{\mathbb{P}} \left(\frac{1}{\sqrt{n}} \right) \quad (\text{EC.2.8})$$

as $m, n \rightarrow \infty$.

For Case 1, first, by the mean value theorem, we have

$$\begin{aligned} & \tau_{j_{m,n}^*} - F_Y(\hat{Y}(\tau_{j_{m,n}^*}|\mathbf{x}^*)|\mathbf{x}^*) \\ &= F_Y(F_Y^{-1}(\tau_{j_{m,n}^*}|\mathbf{x}^*)|\mathbf{x}^*) - F_Y(\hat{Y}(\tau_{j_{m,n}^*}|\mathbf{x}^*)|\mathbf{x}^*) \\ &= f_Y(\eta|\mathbf{x}^*) \cdot \left(F_Y^{-1}(\tau_{j_{m,n}^*}|\mathbf{x}^*) - \hat{Y}(\tau_{j_{m,n}^*}|\mathbf{x}^*) \right) \\ &= \frac{f_Y(\eta|\mathbf{x}^*)}{f_Y(F_Y^{-1}(\tau_{j_{m,n}^*}|\mathbf{x}^*)|\mathbf{x}^*)} \cdot f_Y(F_Y^{-1}(\tau_{j_{m,n}^*}|\mathbf{x}^*)|\mathbf{x}^*) \cdot \left(F_Y^{-1}(\tau_{j_{m,n}^*}|\mathbf{x}^*) - \hat{Y}(\tau_{j_{m,n}^*}|\mathbf{x}^*) \right), \end{aligned} \quad (\text{EC.2.9})$$

where η is between $F_Y^{-1}(\tau_{j_{m,n}^*} | \mathbf{x}^*)$ and $\hat{Y}(\tau_{j_{m,n}^*} | \mathbf{x}^*)$. Therefore, to prove (EC.2.6), it is sufficient to prove that

$$f_Y \left(F_Y^{-1}(\tau_{j_{m,n}^*} | \mathbf{x}^*) | \mathbf{x}^* \right) \cdot \left(F_Y^{-1}(\tau_{j_{m,n}^*} | \mathbf{x}^*) - \hat{Y}(\tau_{j_{m,n}^*} | \mathbf{x}^*) \right) = O_{\mathbb{P}} \left(\frac{\sqrt{\tau_{j_{m,n}^*}}}{\sqrt{n}} \right) \quad (\text{EC.2.10})$$

and

$$\frac{f_Y(\eta | \mathbf{x}^*)}{f_Y \left(F_Y^{-1}(\tau_{j_{m,n}^*} | \mathbf{x}^*) | \mathbf{x}^* \right)} \xrightarrow{\mathbb{P}} 1 \quad (\text{EC.2.11})$$

as $m, n \rightarrow \infty$.

We first prove (EC.2.10). Notice that $\tau_{j_{m,n}^*} \rightarrow 0$ as $m, n \rightarrow \infty$, then $f_Y \left(F_Y^{-1}(\tau_{j_{m,n}^*} | \mathbf{x}^*) | \mathbf{x}^* \right) \rightarrow 0$ as $m, n \rightarrow \infty$. Since m satisfies $\frac{1}{m} \rightarrow 0$ and $\frac{n}{m} \rightarrow \infty$ as $n \rightarrow \infty$, and also $1 \leq j_{m,n}^* \leq m-1$, then $\tau_{j_{m,n}^*}$ satisfies $\tau_{j_{m,n}^*} \rightarrow 0$ and $\tau_{j_{m,n}^*} n = \frac{n}{m} \cdot j_{m,n}^* \rightarrow \infty$ as $m, n \rightarrow \infty$. Therefore, as $m, n \rightarrow \infty$, the sequence $\tau_{j_{m,n}^*}$ is intermediate order quantile levels. Hence by the left-tail version of Lemma 5,

$$f_Y \left(F_Y^{-1}(\tau_{j_{m,n}^*} | \mathbf{x}^*) | \mathbf{x}^* \right) \cdot \left(\hat{\beta}(\tau_{j_{m,n}^*}) - \beta(\tau_{j_{m,n}^*}) \right)^{\top} \mathbf{x}^* = O_{\mathbb{P}} \left(\frac{\sqrt{\tau_{j_{m,n}^*}}}{\sqrt{n}} \right)$$

as $m, n \rightarrow \infty$, which proves (EC.2.10).

We then prove (EC.2.11). Notice that by (EC.2.10), we have

$$\left| F_Y^{-1}(\tau_{j_{m,n}^*} | \mathbf{x}^*) - \hat{Y}(\tau_{j_{m,n}^*} | \mathbf{x}^*) \right| = O_{\mathbb{P}} \left(\frac{\sqrt{\tau_{j_{m,n}^*}}}{\sqrt{n} f_Y \left(F_Y^{-1}(\tau_{j_{m,n}^*} | \mathbf{x}^*) | \mathbf{x}^* \right)} \right) = o_{\mathbb{P}} \left(\frac{\tau_{j_{m,n}^*}}{f_Y \left(F_Y^{-1}(\tau_{j_{m,n}^*} | \mathbf{x}^*) | \mathbf{x}^* \right)} \right)$$

as $m, n \rightarrow \infty$, where the last equality is from $\tau_{j_{m,n}^*} n \rightarrow \infty$ as $m, n \rightarrow \infty$. And notice that η is between $F_Y^{-1}(\tau_{j_{m,n}^*} | \mathbf{x}^*)$ and $\hat{Y}(\tau_{j_{m,n}^*} | \mathbf{x}^*)$, then

$$f_Y(\eta | \mathbf{x}^*) = f_Y \left(F_Y^{-1}(\tau_{j_{m,n}^*} | \mathbf{x}^*) + o_{\mathbb{P}} \left(\frac{\tau_{j_{m,n}^*}}{f_Y \left(F_Y^{-1}(\tau_{j_{m,n}^*} | \mathbf{x}^*) | \mathbf{x}^* \right)} \right) | \mathbf{x}^* \right).$$

Then, the limiting equivalence relationships (9.61) to (9.65) and equation (9.52) of Chernozhukov (2005) show that

$$\frac{f_Y(\eta | \mathbf{x}^*)}{f_Y \left(F_Y^{-1}(\tau_{j_{m,n}^*} | \mathbf{x}^*) | \mathbf{x}^* \right)} = \frac{f_Y \left(F_Y^{-1}(\tau_{j_{m,n}^*} | \mathbf{x}^*) + o_{\mathbb{P}} \left(\frac{\tau_{j_{m,n}^*}}{f_Y \left(F_Y^{-1}(\tau_{j_{m,n}^*} | \mathbf{x}^*) | \mathbf{x}^* \right)} \right) | \mathbf{x}^* \right)}{f_Y \left(F_Y^{-1}(\tau_{j_{m,n}^*} | \mathbf{x}^*) | \mathbf{x}^* \right)} \xrightarrow{\mathbb{P}} 1,$$

as $m, n \rightarrow \infty$. By (EC.2.9), (EC.2.10) and (EC.2.11), we have that (EC.2.6) holds.

For Case 2, by using the right-tail version of Lemma 5, (EC.2.7) may be proved in the same way as (EC.2.6) of Case 1 is proved.

For Case 3, to prove (EC.2.8), again by (EC.2.9), we only need to prove that

$$f_Y \left(F_Y^{-1}(\tau_{j_{m,n}^*} | \mathbf{x}^*) | \mathbf{x}^* \right) \cdot \left(F_Y^{-1}(\tau_{j_{m,n}^*} | \mathbf{x}^*) - \hat{Y}(\tau_{j_{m,n}^*} | \mathbf{x}^*) \right) = O_{\mathbb{P}} \left(\frac{1}{\sqrt{n}} \right) \quad (\text{EC.2.12})$$

and

$$\frac{f_Y(\eta|\mathbf{x}^*)}{f_Y\left(F_Y^{-1}(\tau_{j_{m,n}^*}|\mathbf{x}^*)|\mathbf{x}^*\right)} = O_{\mathbb{P}}(1) \quad (\text{EC.2.13})$$

as $m, n \rightarrow \infty$. Notice that $\tau_{j_{m,n}^*} \in [\varepsilon_1, 1 - \varepsilon_2]$. By Assumption 2, $f_Y\left(F_Y^{-1}(\tau_{j_{m,n}^*}|\mathbf{x}^*)|\mathbf{x}^*\right)$ is uniformly bounded away from 0 for all m, n . Then, (EC.2.12) holds by Proposition 3 and (EC.2.13) holds trivially. Therefore, we have that (EC.2.8) holds.

The analyses of the three cases show that the tails (i.e., Cases 1 and 2) have a faster rate of convergence than the middle interval (i.e., Case 3). By the definition of $j_{m,n}^*$ in (EC.2.5), in the following, we show by contradiction that $j_{m,n}^*$ must be in Case 3. Suppose that there do not exist $\varepsilon_1 > 0$ and $\varepsilon_2 > 0$, such that $\tau_{j_{m,n}^*} \in [\varepsilon_1, 1 - \varepsilon_2]$ when m, n are sufficiently large, that is, for all $\varepsilon_1 > 0$, $M_1 > 0$ and $N_1 > 0$, there exist $m \geq M_1$ and $n \geq N_1$ such that $\tau_{j_{m,n}^*} < \varepsilon_1$; or for all $\varepsilon_2 > 0$, $M_2 > 0$ and $N_2 > 0$, there exist $m \geq M_2$ and $n \geq N_2$ such that $\tau_{j_{m,n}^*} > 1 - \varepsilon_2$. Then, there must exist a subsequence of $\tau_{j_{m,n}^*}$ that falls into either Case 1 or Case 2. However, we have already seen that Case 1 and Case 2 are dominated by Case 3, they do not satisfy the definition of $j_{m,n}^*$. Therefore, we have a contradiction and $j_{m,n}^*$ must be in Case 3.

To sum up, $\tau_{j_{m,n}^*}$ must be in Case 3. Hence, the rate of convergence of $\left|\tau_{j_{m,n}^*} - F_Y(\hat{Y}(\tau_{j_{m,n}^*}|\mathbf{x}^*)|\mathbf{x}^*)\right|$ is $O_{\mathbb{P}}\left(\frac{1}{\sqrt{n}}\right)$. Therefore, by Lemma 6, we have

$$\sup_{y \in (-\infty, \infty)} |F_{\hat{Y}}(y|\mathbf{x}^*) - F_Y(y|\mathbf{x}^*)| \leq \max_{1 \leq j \leq m-1} \left|\tau_{j_{m,n}^*} - F_Y(\hat{Y}(\tau_{j_{m,n}^*}|\mathbf{x}^*)|\mathbf{x}^*)\right| + \frac{1}{m} = O_{\mathbb{P}}\left(\frac{1}{\sqrt{n}}\right) + O\left(\frac{1}{m}\right).$$

This concludes the proof of the theorem. \square

EC.3. Convergence test for CWGAN

We repeat the convergence test of Section 6.1.2 using CWGAN for Scenarios 1 and 2. Because the computational cost of adjusting hyperparameters for these two experiments is too high, we fix `max_epochs` = 1000 and set `batch_size` = $0.2n$ as the tutorial of CWGAN (Athey et al. 2021) suggests that a fraction between 0.1 and 0.5 of n tends to work best. We plot of the results in Figure EC.1. From these plots, we see no clear sign of convergence for CWGAN.

References

- Chernozhukov V (2005) Extremal quantile regression. *Annals of Statistics* 33(2):806–839.
- Resnick SI (2008) *Extreme Values, Regular Variation, and Point Processes* (Springer).
- Dekkers ALM, Haan LD (1989) On the estimation of the extreme-value index and large quantile estimation. *Annals of Statistics* 17(4):1795–1832.
- Athey S, Imbens GW, Metzger J, Munro E (2021) Using Wasserstein generative adversarial networks for the design of Monte Carlo simulations. *Journal of Econometrics*.

Figure EC.1 $\log \bar{D}_n$ v.s. $\log n$ for Scenario 1 and Scenario 2 with CWGAN